JIMMA UNIVERSITY

JIMMA INSTITUTE OF TECHNOLOGY

FACULTY OF CIVIL AND ENVIRONMENTAL ENGINEERING

STRUCTURAL ENGINEERING STREAM

Numerical Analysis of Structural Steel Reinforced Concrete Wall

A thesis submitted to Jimma University, Jimma Institute of Technology, Faculty of Civil and Environmental Engineering in the partial fulfilment for degree of masters science in civil engineering (speciality in Structural Engineering).

By:

Yehamleshet Menberu

February, 2018

JIMMA, ETHIOPIA

JIMMA UNIVERSITY

JIMMA INSTITUTE OF TECHNOLOGY

FACULTY OF CIVIL AND ENVIRONMENTAL ENGINEERING

STRUCTURAL ENGINEERING STREAM

Numerical Analysis of Structural Steel Reinforced Concrete Wall

A thesis submitted to Jimma University, Jimma Institute of Technology, Faculty of Civil and Environmental Engineering in the partial fulfilment for degree of masters science in civil engineering (speciality in Structural Engineering).

By:

Yehamleshet Menberu

Main advisor : Dr. Temesgen Wondimu

Co advisor: Haymanot Gebresilassie(Msc)

February, 2018

JIMMA, ETHIOPIA

DECLARATION

This thesis is my original work and has not been presented for a degree in any other University

YehamleshetMenberu:

Signature________________ Date_______________

I will submit this proposal for examination with my approval as University Supervisor

Advisers

Main adviser: Dr. TemesgenWondimu

Signature______________ Date ________________

Co adviser: HaymanotGebresilassie

Signature ________________ Date_________________

JIMMA UNIVERSITY

JIMMA INSTITUTE OF TECHNOLOGY

FACULTY OF CIVIL AND ENVIRONMENTAL ENGINEERING

STRUCTURAL ENGINEERING STREAM

Numerical Analysis of Structural Steel Reinforced Concrete wall

A thesis submitted to Jimma University, Jimma Institute of Technology, Faculty of Civil and Environmental Engineering in the partial fulfillment for Degree of Masters of Science in Civil Engineering (Structural Engineering).

By:

YEHAMLESHET MENBERU

JIMMA INSTITUTE OF TECHNOLOGY

Dr. TEMESGEN WONDIMU	______________	________________
(Main Advisor)	Signature	Date
HAYMANOT GEBRESILASSE(MSc.)	____________	______________
(co- Advisor)	Signature	Date

Approved by Board of Examiners

_____________________	______________	______________
(External Examiner)	Signature	Date
_____________________	______________	______________
(Internal Examiner)	Signature	Date
____________________	________________	______________
(Chairman)	Signature	Date

Acknowledgment

My first and foremost gratitude goes to Almighty God who is always there for me through the times of trouble and good times.

I would like to express my gratitude to my husband, families and friends for their unrelenting and rigorous moral support not only on my educational careers but throughout my life.

I would also like to thank my main advisor Dr.TemesgenWondimu and co- advisor Haymanot Gebresilassie for their valuable advice and guidance during this thesis work.

Finally, my special thanks goes to Jimma Institute of Technology for facilitating this program which helped me for upgrading my profession.

Abstract

A nonlinear finite element analysis is performed for axialy and laterally loaded structural steel reinforced concrete walls. Since simulating this kind of stuctures in ABAQUS is difficult, several simulations are made to find the correct model with satisfying accuracy. Both geometric and material nonlinearities are included in the Finite Element model; a concrete damage plasticity model capable of predicting both compressive and tensile failures is used.

Numerical simulation is compared with the experimental results published by other researchers. The Simulation responses agree well with the corresponding experimental results for predicting the load carrying capacity, ductility and failure mode of Structural Steel Reinforced Concrete (SRC) walls but the hysteresis loop became a little off due to a limitation of material models integrated in ABAQUS 6.13.

Using the developed model, parametric study is conducted to investigate the effect of structural steel shape, axial load ratio, aspect ratio and concrete grade on the load carrying capacity of wall and also sensitivity analysis have been done for the selected 5 parameters, which include thickness of wall and structural steel flange thickness for geometic parameters, and yield strength of structural steel, yield strength of reinforcement bar and concrete grade for material strength parameters. A total of 56 models have been used to do the parametric study.

The result shows structural steel with channel shape exhibit high load carring capacity , high axial load ratio results in high load resistant but lessr ductility, aspect ratio has an inverse relation ship with capacity. Concrete grade has a direct relation with the capacity of the wall but does not have any effect on the ductility and failure mode of the shear wall which most likely is because of the failure of concrete at early stage making contribution of the concrete less for ductility.

From the sensitivity analysis, the most sensitive parmeter found in this study is thickness of flange of structural steel from geometric parameters and yield strength of structural steel from the material strength parameters.

Key words: *Slender, Shear wall, Structural wall, Structural steel, Reinforced concrete,*

Table of Contents

List of Tables

List of Figures

Acronyms and Abbreviations

ACI	Americal Concrete Institute
FEM	Finite Element Method
JIT	Jimma Institute of Technology
RC	Reinforced Concrete
SRC	Structural Steel Reinforce Concrete
ε_{Cu}	Ultimate Compressive strain of concrete (mm/mm)
A_g	Gross Area of Concrete (mm^2)
f_c'	Concrete Compressive Strength (MPa)
f_y	Steel Yield Strength (MPa)
E_c	Modulus of Elasticity of concrete (MPa)
ε_{cr}	Cracking tensile strain of concrete (mm/mm)
E_{cm}	Secant modulus of elasticity of concrete (MPa)
f_{ct}	Concrete Tensile Strength (MPa)
ε_c^{-in}	Inelastic strain mm/mm
ε_c^{-pl}	Plastic Strain mm/mm
d_t	Damage parameter in tension
d_c	Damage parameter in compression

CHAPTER ONE

INTRODUCTION

1.1. General

Reinforced concrete structural walls are deep and relatively thin, vertical cantilever members, also referred to as “shear walls”. Structural walls are widely used in reinforced concrete buildings located in earthquake-prone regions as the primary lateral-load resisting mechanism, because of their efficiency to provide lateral strength and stiffness, and control the lateral drift.

Structural walls can be found in various shapes and sizes, with different configurations in the building plan. Symmetrical sections, for example rectangular and barbell shaped, are quite frequent, although “flanged”, asymmetrical wall sections such as T- and L-shaped sections are also often used. The effect of the wall cross-section shape on the seismic behavior of a shear wall has been investigated by several researchers and it has been shown that the wall strength, stiffness, and ductility depend greatly on the shape of the wall (Paulay, 1986(a); Wallace and Moehle, 1989). One of the most common classifications of structural walls is with respect to their overall height-to-length ratio (wall aspect ratio). Walls with aspect ratio greater than two are usually referred to as “slender walls” and have a behavior mainly dominated by flexure. Slender walls are quite common in tall buildings because of their efficiency in resisting lateral loads and limiting lateral drift. Structural walls with an aspect ratio smaller than two are usually called “low-rise” walls, where shear tends to govern the overall wall response. “Squat walls” are typically defined as walls with an aspect ratio smaller than one. Low-rise walls find application in residential buildings, parking structures, industrial buildings, nuclear power plants, and also in highway overpasses and bridge abutments.

The philosophy often used in the design of concrete walls focuses on providing the required strength and stiffness to avoid or limit damage under frequent earthquakes (limited or no inelastic behavior) while ensuring sufficient wall deformation capacity so that the lateral load capacity can be maintained during the inelastic response expected during stronger, less frequent earthquakes (Massone and Wallace, 2004). Structural walls must also be able to dissipate energy after yielding to survive strong ground motions and should not be susceptible to sudden failures due to shear or local instabilities (Pauley et al., 1982)

To resist the majority of the tension and compression forces that develop under the applied lateral loads at wall edges (boundary elements) flexural reinforcement is concentrated at these areas, with lighter flexural reinforcement typically used within the wall web between the boundary zones. According to ACI-318(99) transverse reinforcement must enclose the boundary longitudinal reinforcement, which typically consists of a relatively large number of large diameter reinforcing bars, to confine the core concrete and to restrain buckling of longitudinal reinforcement. Replacing the majority of the boundary vertical reinforcement (longitudinal reinforcement) is a promising alternative construction approach which avoids congestion created by the relatively large quantities of longitudinal and transverse reinforcement at wall boundaries as well as the anchorage of horizontal web reinforcement at the wall boundary. This technique of embedding a structural shape within concrete is commonly referred to as structural steel reinforced concrete wall (SRC) construction.

Use of an SRC system may offer several advantages. For example the embedded steel sections at the boundary may not be susceptible to buckling as reinforcing bars, and might also delay buckling of the supplemental deformed longitudinal boundary reinforcement (in addition to the structural steel section), leading to an improved behavior relative to RC construction. SRC system may also promote rapid and ease of construction, since structural steel boundary columns could be used to support formwork and construction loads for several levels above the level reached for concrete placement. (Leonardo et.al,2017)

Because of the several advantages gained from this system, it became an attractive alternative but observations shown that several potential problems exist. As Roader Cw , The embedded steel section may slip due to lack of sufficient bond stress or encased steel section may act like a wedge and split the surrounding concrete thereby reducing the effective nominal flexural strength. Also, it has been observed that the restraint against lateral expansion provided by encased steel sections can cause vertical web splitting along the interface between the embedded steel section and the wall web. (Leonardo et al, 2017)

Since SRC walls are a new technology, further investigation is needed to examine the behavior of these walls for different parameters. Currently, different studies have been conducted experimentally and numerically to study the performance of these walls under the conventional

RC walls. This study numerically analyse Structural Steel Reinforced Concrete walls to investigate the behavior of these walls for different parameters.

1.2. Statement of the problem

Structural steel reinforced concrete wall became the most effective lateral load resisting system around the world specially on earthquake prone areas.Since it is necessary to understand the behavior of these walls,different experimental studies have been conducted to investigate the responses of composite walls with different parameters, i.e., axial load, cross sectional shape, location of the steel cross-section and other parameters but there is still a limited knowledge on the behaviour of these walls subjected to axial and lateral load for composite walls with out shear stud.

Considering the cost and time to undertake full-scale experimental investigation on SRC walls, this study conducts a finite element (FE) analysis for SRC wall to investigate the behaviour of SRC wall subjected to both axial and lateral loadings to show the effects of structural steel shape used at the boundary, axial load ratio, aspect ratio of the wall and concrete grade.

1.3. Objectives

1.3.1 General Objective

The main objective of this study is to conduct a nonlinear finite element analysis of Structural Steel Reinforce Concrete walls walls under gravity and cyclic lateral loading and validate it with experimental result of Leonardo et al and investigate the effect of different input parameters on the behavior of walls under both gravity and cyclic loading using finite element software package ABAQUS.

1.3.2. Specific Objective

- To develop finite element model which is capable of simulating the behavior of SRC walls.

- To investigate the effect of structural steel shape, axial load ratio, aspect ratio and concreter grade on the load carrying capacity, ductility and failure mode of Structural Steel Reinforced Concrete wall using ABAQUS 6.13.
- To perform sensitivity analysis and select the most sensitive parameter from the parameters under study.

1.4. Research question

- How does the shape of structural steel, axial load ratio , aspect ratio and concrete grade affect the load carrying capacity, ductility and failure mode of Structural Steel Reinforced Concrete wall ?
- Which parameter is the most sensitive parameter?

1.5. Scope of the study

The main part of this study deals with the modeling of response of Structural Steel Reinforced Concrete wall subjected to axial and cyclic loading. The effect of structural steel shape, axial load ratio, aspect ratio and concrete grade has been considered and sensitivity analysis has been done for rectangular shear walls. Other shapes of shear walls are out of the scope of this study.

1.6. Expected outcome

Simulation is becoming a good approach to study the responses of different structures and different researchers proved this. In this research it is expected to get a detailed behavior of walls under the subjected loads which can help to identify the effects of selected parameters on the behavior of the walls.

1.7. Significance of the study

Since it is very expensive and time taking to conduct large scale experimental tests this research helps to examine the behavior of SRC walls using numerical analysis. This analysis helps to investigate the behavior of SRC walls under both gravity and cyclic loads which helps to investigate the behavior of SRC walls. Also will help to select appropriate shape of structural steel, size of wall and load level during design. Finally it helps to identify the most sensitive parameter so that care should be given for that parameter while measuring.

CHAPTER TWO

LITERATURE REVIEW

2.1. General

Due to their high initial stiffness and lateral load carrying capacity, shear walls are an ideal choice for a lateral load-resisting system in RC structure. The stiffness of an RC component depends on material properties, component dimensions, reinforcement quantities, boundary conditions, and stress levels. Because of large number of reinforcement used for shear walls it creates congestion at the boundary and complicates construction. Hence, SRC method is the best solution to overcome the problems and different studies have been conducted to investigate the performance of this method.

Different types of composite shear wall systems have been studied for the purpose of improving the ductility of the conventional reinforced concrete shear walls. Recent research on composite shear walls were conducted by Liaonardo et al., Dan et.al, Zhou et al. and Lu and Yang experimentally. Numerical investigation was done by Daniel et al.

2.2. Studies on composite shear walls

According to Leonardo et al.(2017) experimental results conducted for three SRC walls (SRCW1, SRCW2, SRCW3) with aspect ratio (AR=hw/lw) of 4 for all specimen. The structural steel used at the boundary for SRCW1 and SRCW3 is the same which is W16×9 and have different number of reinforcement bars at the boundary and for SRCw2, W6×16 is used at the boundary and equal number of reinforcement bar was used with SRCW1. SRCW1 and SRCW2 loaded by constant axial load of $0.10A_gf_c$’ and 0.18 A_gf_c’ for SRCW3 and a cyclic lateral displacement. SRC walls presented good behavior regarding strength. All specimens were able to reach the design drift level (1.5%) without strength loss . beyond 2% lateral drift SRCW1 shows 45% strength loss, SRCW2 shows 20% strength loss and no strength loss on SRCW3 until about 2.5% lateral drift but out-of-plane failure is observed once. Regarding the effect of slippage of steel section on the behavior of the wall, the result shows slippage reduces the stiffness of the wall approximately by a factor of two. From the results the researchers recommended to provide at least 70% of the bond strength by structural steel embedment in order to promote yielding. The result shows that, increase in structural steel size increases the stiffness of the wall but a better performance of the wall can be found by increasing the quantity of reinforcement bar without changing the size of cross-sectional steel at the boundaries. (Leonardo et.al, 2017). The figures below shows failure modes of the wall(SRCW1).

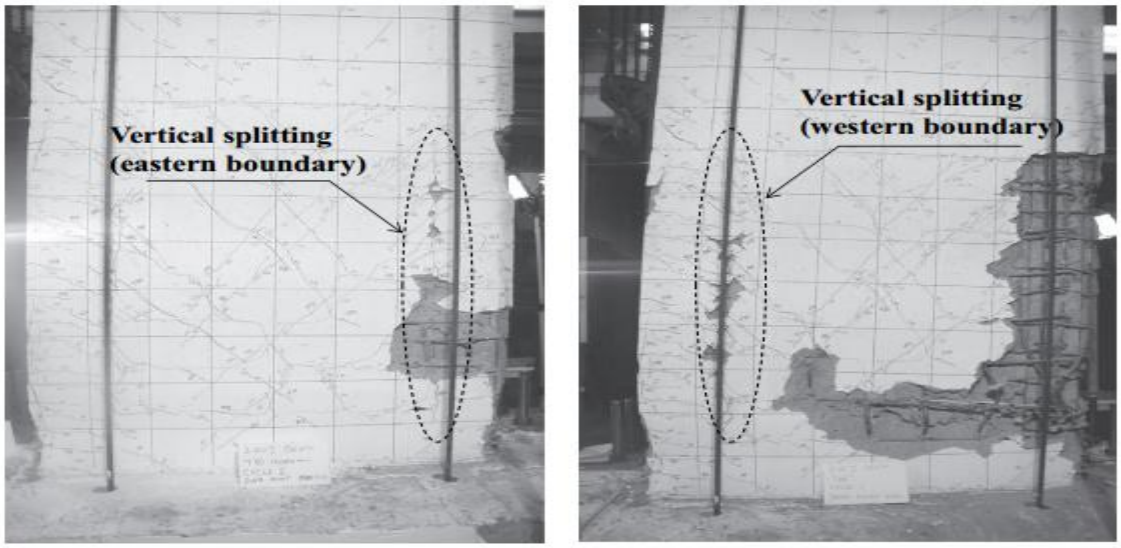

(a) (b)

Figure 2. 1: Failure of concrete on specimen SRCW1 (a). at 2.5% storey drift (b). at 4% strorey drift (Leonardo et.al, 2017)

(a) (b)

Figure 2. 2: Failure of steel (a). Fractured bar (b). Buckeled bar at 3% storey drift (Leonardo et.al, 2007)

D.Dan et al (2011) tested 5 shear walls with steel encased profiles and 1 reinforced concrete typical shear wall .All the specimens had the same amount of vertical reinforcement. The study investigated the effects of type of vertical side reinforcement (reinforcement bars or structural steel, position of structural steel in the cross section). The structural steel profiles were connected with the concrete web by headed shear stud connectors with d = 13 mm diameter and h = 75 mm length. The specimen CSRCW3 had a supplementary steel encased profile placed in the middle of the cross section. For all specimens the reinforcements of the RC web panel consists of Ø10/100mmvertical bars and Ø8/150mmhorizontal bars. Vertical and horizontal reinforcements were placed on both faces of the wall and were connected together with Ø8/400/450 mm steel ties. For specimen CSRCW5, the horizontal bars were welded on the steel profiles. All specimens are loaded under constant vertical load and cyclically increasing horizontal (lateral) loads. The result showed that composite wall had a higher initial stiffness than the reinforced concrete wall. The value of the element stiffness prior to failure is higher for the composite wall than for the reinforced concrete wall.

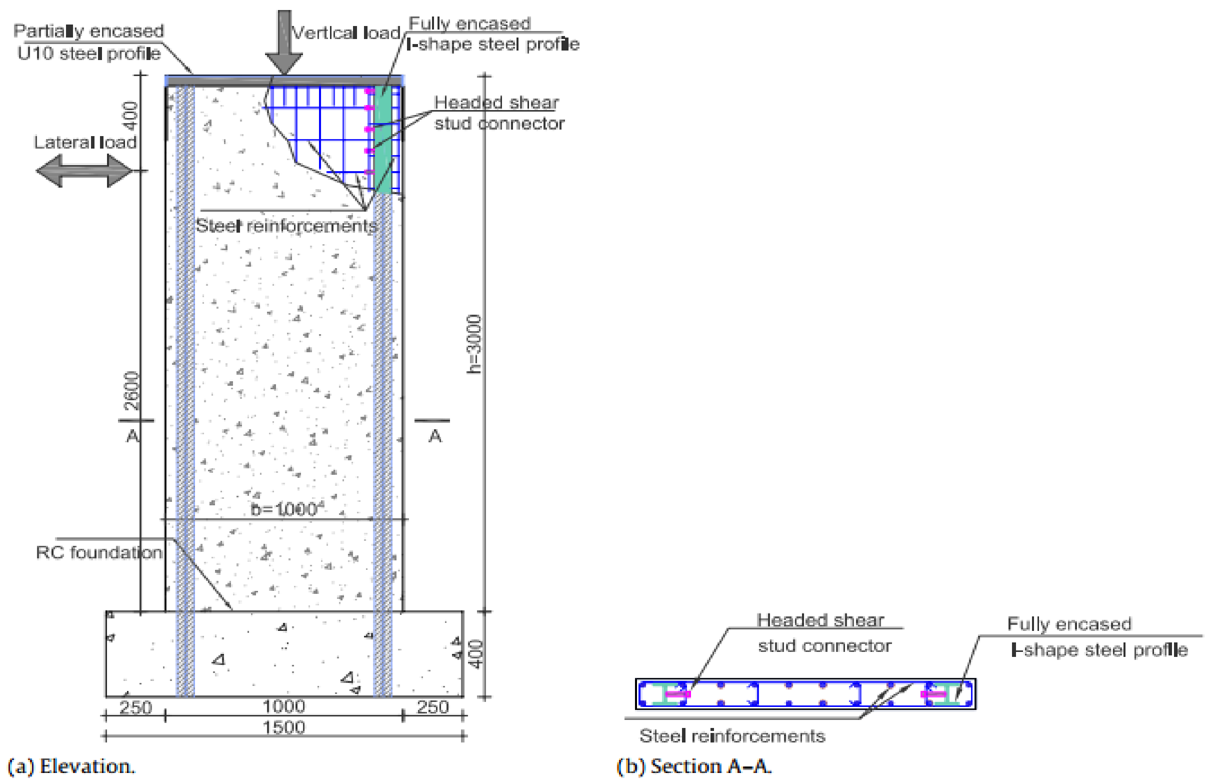

Figure 2. 3: Composite Steel-Concrete Experimental element(D.Dan et.al.,2011)

M.A. Osman et al.(2011) investigated the behavior of I-section RC walls to identify the effect of height-to-width ratio and the compressive strength of concrete under a constant axial load and reversal increased loading as shown in figure 2.4 until failure. The result indicate the lateral load carrying capacity and the stiffness of the wall is high for high strength concrete than the normal strength concrete while the ductility index decreases. A significant increasing of the stiffness was observed for small height to width ratio. Regarding the failure mode for high strength long wall as shown in figure 2.5. the failure mode was flexural-shear failure but for high strength short walls it was shear failure.

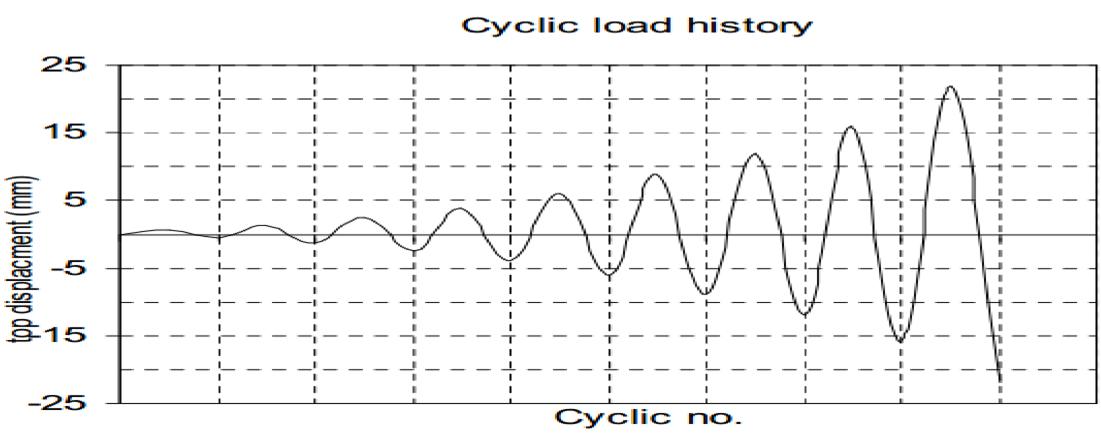

Figure 2. 4: Cyclic load history used for the test (M.A. Osman et al.,2011)

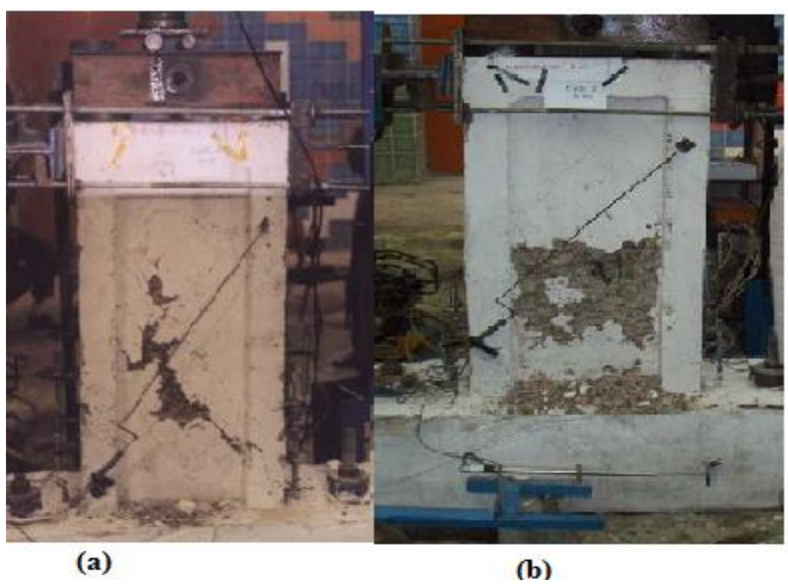

Figure 2. 5: Crack Patterns (a) specimen HL1 and (b) Specimen HL2 (M.A. Osman et al.,2011)

Jiaru Q. et.al.(2012) experimentally tested the behavior of steel tube reinforced concrete walls subjected to high axial force and cyclic loading for examining the contribution of area ratios of steel tubes and CFSTs over that of the wall boundary element, axial force ratio and cross-sectional shape of walls on the load-carrying and deformation capacities of ST_RC walls. The study clearly showed composite walls have larger load-carrying and deformation capacities than RC wall counterpart. The barbell-shaped composite wall that was configured with edge columns had much larger deformation and energy dissipation capacities than the rectangular shaped walls. The deformation capacity was directly related to the area ratios of steel tubes and CFST and inversely related with the axial load for rectangular shaped composite walls.

Daniel et.al.(2009) made numerical analysis of composite shear wall using BIOGRAF software. Six proposed 1/3 scale elements were modelled to predict non-linear behaviour ,stress distribution along the cross section of the elements, crack distribution, structural stiffness at various loads, load bearing capacity of different types of composite steel–concrete shear walls, The differences between the six proposed element types are due to the arrangement of the steel shapes on the cross section of the wall and also due to the shape of the steel encased element. All six elements have a 3,000 mm height, 1,000 mm length and 100 mm depth. The encased steel profiles are 70 × 70 × 5 mm squared tubular sections, welded wide flange sections 70 × 70 × 5 × 7 mm, 100 × 70 × 5 × 7 mm. The steel profiles are connected with the concrete by Ø13 mm headed shear stud connectors with 60 mm length. The reinforcement is made by vertical bars having Ø10/100 mm and horizontal bars of Ø8/150 mm. The confinement zones are made by Ø8/150 mm stirrups which hold together the longitudinal reinforcements from the ends of the elements. Both vertical and horizontal reinforcements are placed on both sides of the concrete wall and connected together with ties having Ø8/400/450 mm. Element CSRCW-6 is a traditional reinforced concrete shear wall and it is designed to have the amount of reinforcement concentrated at the end approximate to steel amount from other elements. The concrete used is C20/25 class, the reinforcements are made by steel S355 and the structural steel is Fe510. The elements are considered cantilevers subjected to horizontal loads applied as incremental loads, in the nodes from the top of the mesh. The result shows that the maximum shear force obtained at element CSRCW-3 which has an encased profile at the middle of the cross section. So it can be noticed that the amount of steel in composite shear wall cross sections influences the value of ultimate shear force. Also for element CSRCW-6, which is the ordinary reinforced concrete, is observed it has the lowest shear capacity although the amount of vertical reinforcement is equal to the amount of steel from the encased element.

Ying Zhou. et.al.(2010) tested 16 SRC 1/3 scale cantilever wall specimens subjected to a point cyclic lateral load and constant axial load between 0.09fcAg and 0.24fcAg. Wall aspect ratios (AR) ranged from 0.8 to 3.75, with four, slender wall tests (AR 2). Primary test variables were aspect ratio and axial load, with test specimens designed to match the amount of reinforcement that would exist for the same walls designed with traditional longitudinal reinforcement. Test results were consistent with expectations for specimens with traditional reinforcement, specimens with smaller aspect ratio or larger axial load yield reduced ductility

Hong-Song et.al. (2016) experimentally investigate the sesmic behavior of thre Concrete-filled steel tube-enhanced steel plate-reinforced concrete (CFST-SPRC) shear wall for varying steel plate thnicness and concrete strengths. The walls were tested under constant axial force and reversed cyclic loading. All of the specimens experienced a progression of failure from web concret cracking, to local buckling of the steel tube plates to fracturing of the vertical welds at the corners. One specimen exhibited brittle failure at the end of the testing due to sudden crushing of web concrete (SRCW-2). It is observed for the experimental test that CFST-SPRC shear walls have a stable and full hysteretic behavior which indicate a capability for stable energe dissipation. Parameters of the specimens are shown in table 1.1.

Table 2. 1: Parameters of specimen (Hong-Song et.al., 2016)

Specimen designation	f_{cu} (N/mm^2)	Steel plate thickness (mm)		Steel content ratio	Axial compressive force (kN)
		Boundary element	Wall web		
SRCW-1	67.3	5	10	7.1%	6533
SRCW-2	87.8	5	10	7.1%	7877
SRCW-3	83.3	3	6	4.6%	7000

The above literature review indicates that the behavior of shear wall with structural steel under various types of loading, the position of structural steel, the detailing of boundary elements for different shape of structural steel used. The review shows that the new mechanism of embedding structural steel at the wall boundary has showed good result on the behavior of these shear walls for different parameters. However, the review indicates insufficient information regarding the shape of structural steel embedded. Hence in this investigation an attempt has been made to understand the behavior of shear wall for different shape of structural steel at the boundary for different aspect ratios.

2.3. Finite element Method

FE model can predict the behaviour of the composite shear walls with reasonable precision. Stress and strain analysis can be done using FE model to investigate the load transfer mechanism of the composite shear walls. Parametric studies can also be done to identify the influence of different parameters on the performance of the RC shear wall with SRC boundary columns. (FEi-Yu Lio, 2012)

The FEM is essentially a generalization of standard structural analysis procedures which permit the calculation of stresses and deflections in two- and three-dimensional structures by techniques similar to those used in the analysis of ordinary framed structures. In this method, the structure is assumed to consist of a finite number of elements, interconnected at a finite number of Joints or nodal points. All of the material properties of the original system are retained in the individual elements. The method provides a unified approach by which any type of structural configuration may be analyzed.

2.4. Studies on Finite Element Modeling of Concrete Structural Elements

Ahmed et al. (2013) carried out work on finite element modeling of nonlinear cyclic behavior of I-shaped composite steel-concrete shear walls of nuclear power plants. A three-dimensional finite element model was developed to examine the structural behavior of the Composite shear wall under cyclic loading conditions. Nonlinear finite element analysis was performed using the ABAQUS program. First order reduced integration three dimensional eight node solid element (C3D8R) is used for both concrete and steel plate, the model is fixed at the bottom to restrain each component of shear wall in all degrees of freedom and to simulate the prototype. Element mesh and interface element configuration used for the simulation is shown in figure 2.6 below. The loading is applied as a displacement control scheme rather than load control scheme to generate cyclic behavior of composite steel-concrete shear wall by defining smooth amplitude which represents the total history data. Concrete damage plasticity is from ABAQUS material library to model the nonlinear behavior of concrete. The result has been validated with the experimental results and it shows a good correlation, the model best described the monotonic behavior of composite steel-concrete shear wall.

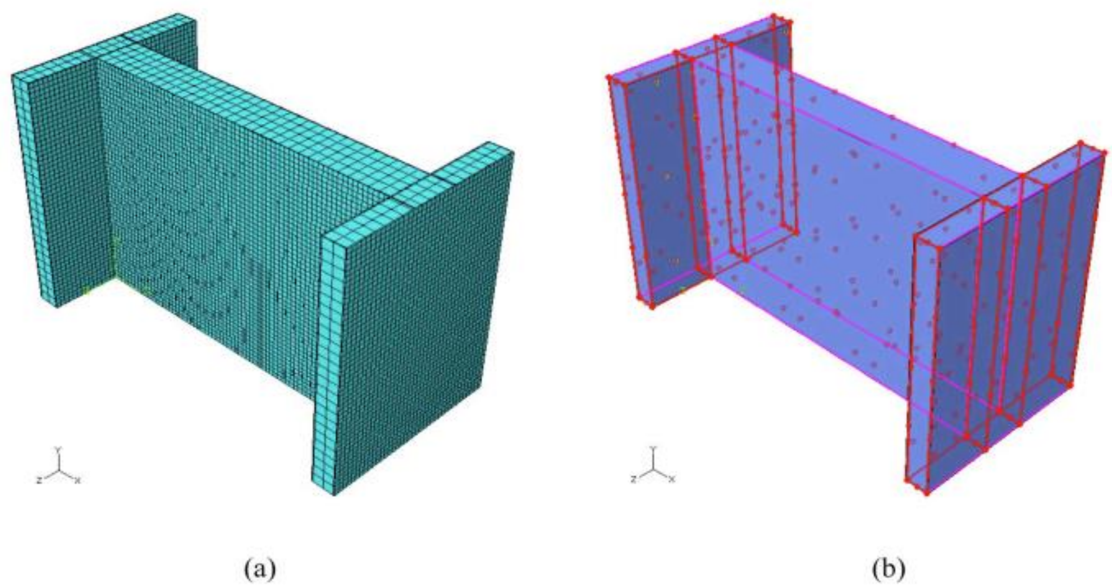

Figure 2. 6: (a) Element Mesh and (b) Interface Element Configuration adopted for simulation Ahmed et al. (2013)

Fei-Yu.Liaoet.al.(2012) developed a finite element (FE) model to simulate the behavior of Reinforced Concrete shear wall with steel Reinforced boundary column (SRC–RC) walls under constant axial load and lateral loading. A series of tests, including six shear wall specimens, were conducted under cyclic loading condition to investigate the strength, ductility and energy dissipation of them, as well as to verify the FE model. The result shows that FE result have a good correlation with the experimental test and can validate. The research also investigates the load transfer mechanism using FE model and carries out a parametric analysis for SRC-RC walls. From the result the following conclusion were made, the lateral load-carrying capacity of SRC–RC walls increases with increasing axial load level or decreasing height–width ratio, whilst the effects on the ductility and energy dissipation are the reverse.

MA.Osman (2013) have done nonlinear three dimensional finite element models to investigate the cumulative damage of composite columns subjected to cyclic loading for different levels of axial loads on the cyclic capacity of steel, reinforced concrete and composite beam-columns using ABAQUS software. For material modeling concrete damage plasticity was used for concrete and elastic-plastic for structural steel section and reinforcement bars to consider the nonlinear behavior. The loading was done as force controlled for the first three cycles and displacement control for the remaining cycles. Three dimensional eight node reduced integration is used. Comparison has made with the experimental result to validate the model and shows a good correlation. This research also conduct a parametric study to see the effect of axial load on the cyclic behavior of composite beam-columns by assessing the elastic stiffness, high stress and strain zone and evaluating the effects of the level of axial load on stiffness, strength and ductility of beam-column prototypes.

In this section, the finite element modeling of reinforced concrete elements using different packages, and their comparison with experimental investigations are reviewed. Considering the capabilities of the finite element software package ABAQUS, the same was adopted for the present work.

CHAPTER THREE

METHODOLOGY

3.1. Research Design

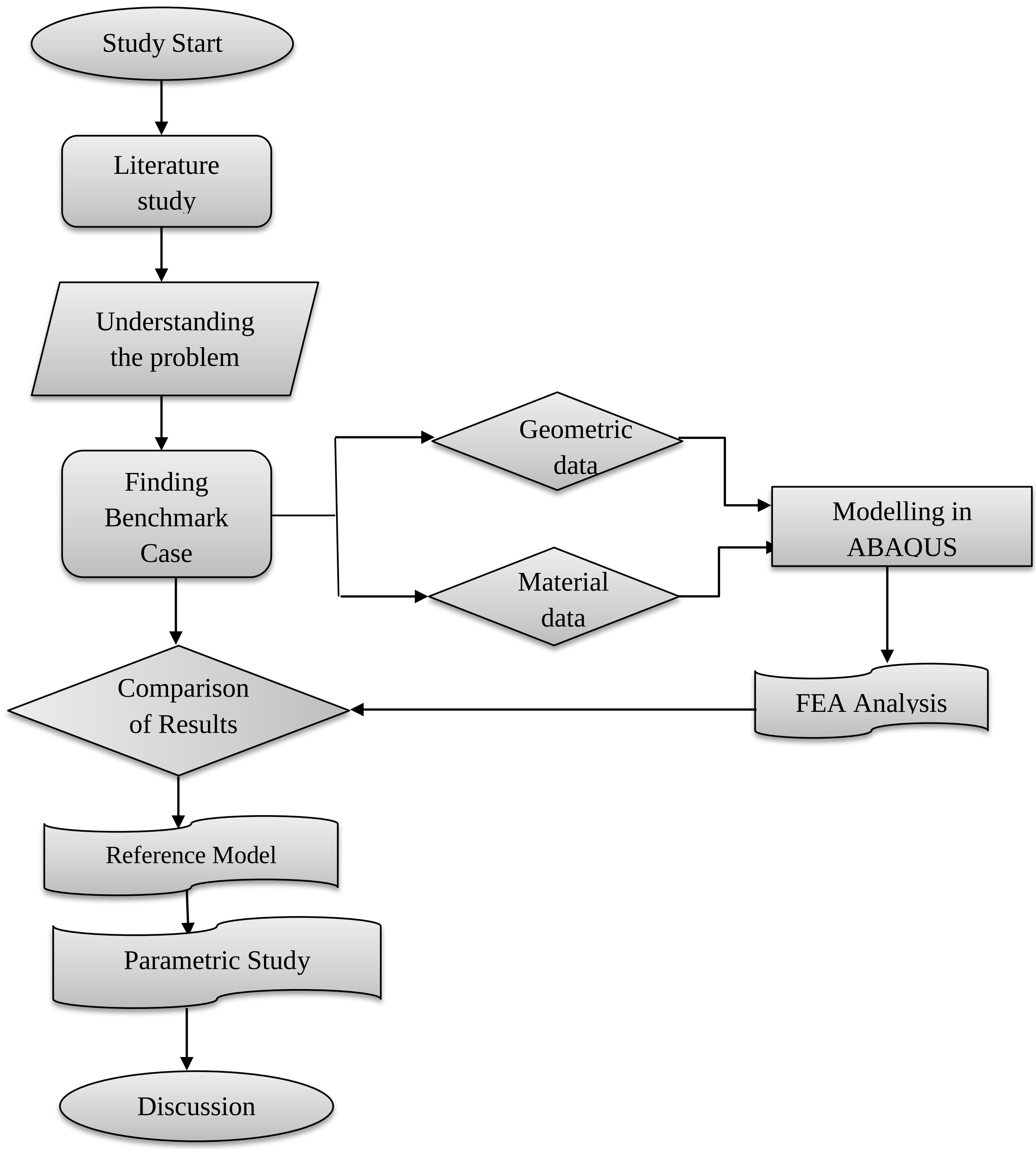

Figure 3. 1: Work Flow

3.2. Finite Element Model of Structural Steel Reinforced Concrete Shear Wall

Experimental studies do not cover the full range of cases that might be encountered in practice as it is too much expensive. It is therefore, necessary to develop analytical tools to investigate the behavior of structural steel reinforced concrete shear walls with different geometry and loading conditions, thus avoiding the large expense of performing additional tests. The chapter describes the development of a finite element model that can simulate the behavior of Structural Steel Reinforced Concrete shear walls under cyclic loading. Experimental model of Leonardo et al (2017) is adopted as a reference test specimen for finite element modeling with the help of general-purpose nonlinear finite element program ABAQUS 6.13.This software is well suited for the solution of highly nonlinear engineering problems. It contains an extensive library of elements that can model virtually all geometric boundary conditions (Hibbitt et al. , 2001).

3.3. Description of Reference Test specimen Leonardo et al. (2017)

A schematic of the experimental model of Leonardo et al (2007) are shown in Figure 3. 1. The prototype building used to help the design of the test specimens is a typical 15-story office building loacated in UBC-97 zone 4 on a stiff soil. The design was based on Rw=8 and an estimated fundamental period of 0.98 seconds. The test specimens are approximately one-third scale replicas of the prototype walls. The specimen is 152mm thick and 1.22m long cross-sections and the height between the application of lateral load near the top of the wall and the critical section at the base of wall is 4.88m.

Plan view of the sample at two heights (lower and upper section)

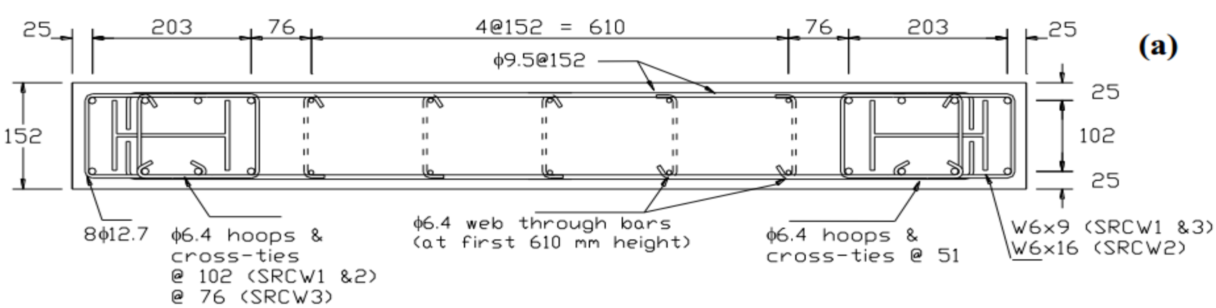

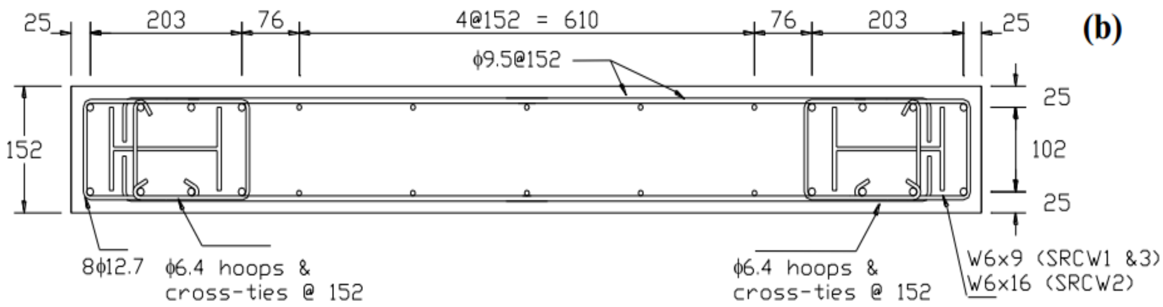

Figure 3. 1: Rectangular wall section: (a) Plastic hinge region (lower 1270mm) (b) Upper section. Dimensions are in mm (Leonardo et.al., 2017)

Elevation View

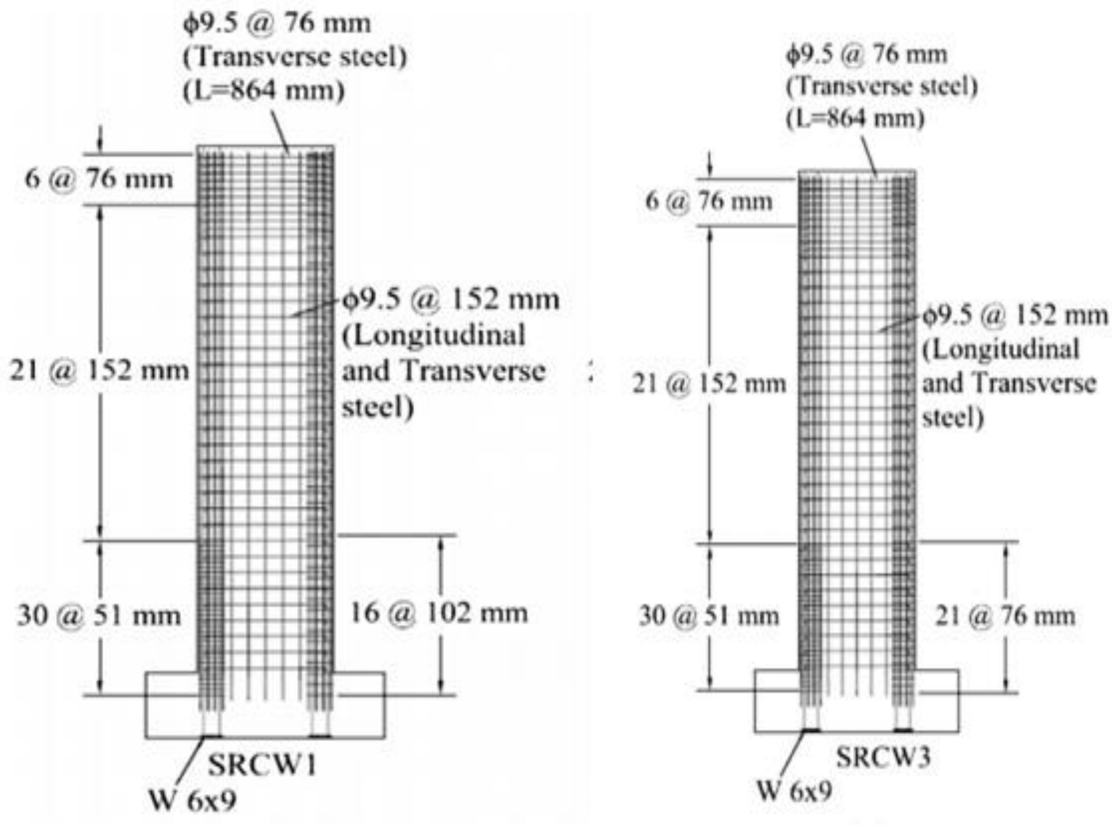

(a). SRCW1 **(b). SRCW3**

Figure 3. 2: Elevation of specimen with steel distribution (Leonardo et.al, 2017)

Wall Boundary Detailing

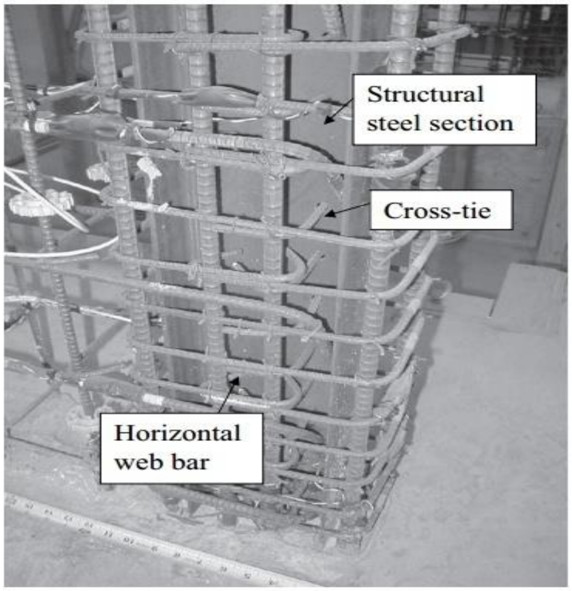

Figure 3. 3: Wall boundary detailing (Leonardo et.al, 2017)

The wall height to wall length ratio (h_w/l_w) = 4 and the primary longitudinal reinforcement at the wall boundary consists of $W6\times9$ (Structural steel A=1729mm^2) section surrounded by 8 ≠ 4 longitudinal bars as a secondary boundary vertical reinforcement and also helps as a support for the transverse reinforcement used at the wall boundaries. To anchor the test specimen to the strong floor a 25mm thick, 127mm by 203 mm base plate was attached to the base of each steel section and embedded in a support block at the base of the wall.

The web reinforcement consisted of two curtains of $\neq 3$ deformed bars spaced at 152mm on center in both the vertical and horizontal directions, terminated with 90 degree hooks. For cross ties, holes were drilled in the web of the structural steel boundary columns. $\neq 2$ deformed bars were used for hoops and crossties. The vertical spacing of the hoops/crossties was 51mm and continued from the wall base to a height of 1.27 m above the base based on an assumed upper-bound plastic hinge length which is equal to the wall length. Above this region the vertical spacing of the hoops increased to 152mm. crossties were provided along the web over the bottom 0.61m of the wall.

Table 3. 1: Geometric properties of refrence test specimens

Specimen Disignation	tw (mm)	Lw (mm)	Hw (mm)	Structural steel	Reinforcement			
					Boundary Longtidunal Reinforcement	Web Longitudinal reinforcement	Transverse reinforcement	Crossties
SRCW1	152	1220	4880	$W6\times9$	$8\phi12.7$	$\phi9.5@152$	$\phi9.5@152$	$\phi6.4@102$
SRCW3	152	1220	4880	$W6\times9$	$8\phi12.7$	$\phi9.5@152$	$\phi9.5@152$	$\phi6.4@76$

Specimen SRCW1 and SRCW3 were subjected to a constant axial load of 0.10Agf$_c$' (641kN) and 0.18A$_g$fc' respecitively and cyclic lateral displacements were applied to the walls by a hydraulic actuator mounted horizontally to a reaction wall 4.88 m above the wall. Out-of-plane support was provided to prevent twisting of the wall specimen during testing. The specimen was subjected to two complete cycles of the following drift levels: 0.10 %, .25%, 0.5%, 0.75%,1%,1.5%,2%,2.5%,3% and 4% as recommended by FEMA 356. The wall test setup is shown in figure 3.5.

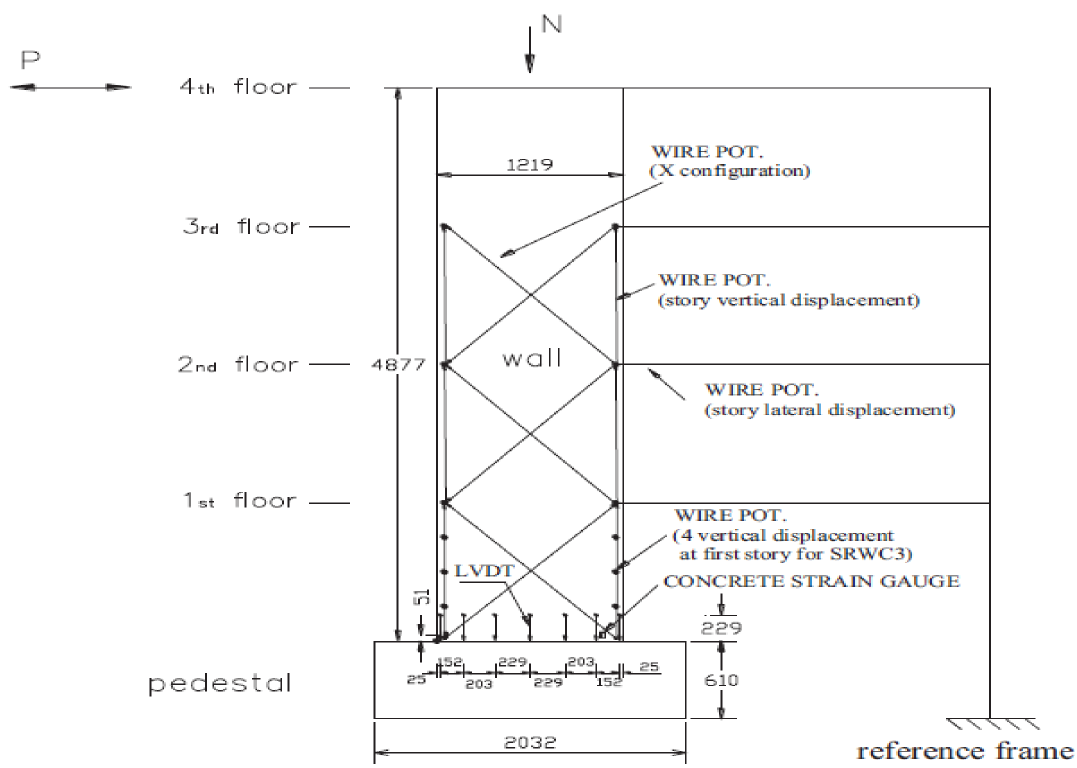

Figure 3. 4: Test setup

3.3.1. Material Properties used

The structural steel sections (W6x9) were A572, Grade 50. The stress vs. strain relations for steel coupons obtained from the steel sections were tested according to ASTM A370-97 . The average concrete compressive strength used for shear wall specimens was 34.5 MPa;

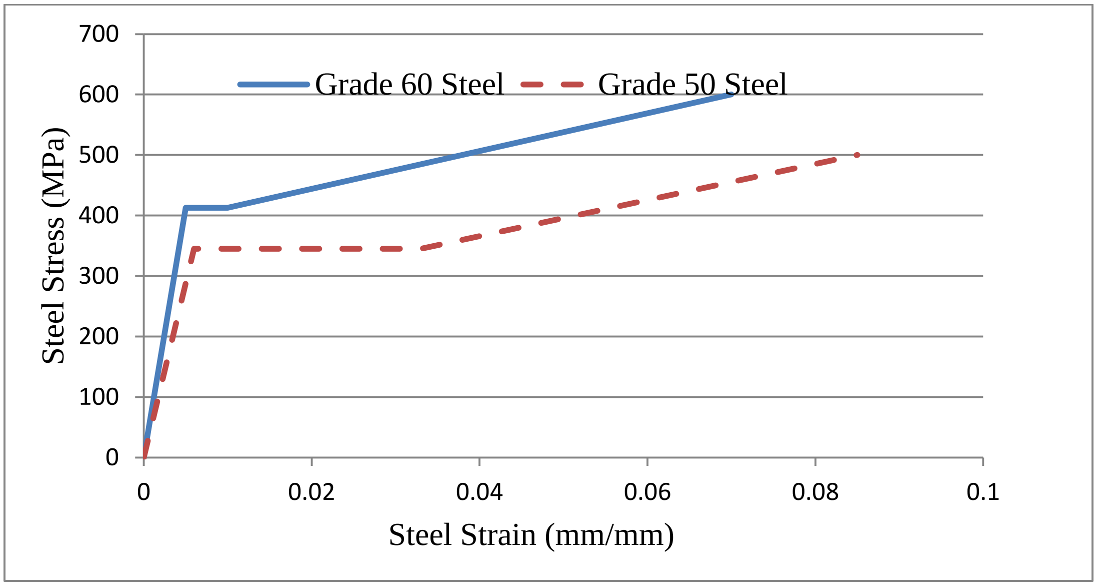

Figure 3. 5 Stress Strain Diagram for steel (Leonardo et.al, 2017)

3.4. Description of finite element model

3.4.1. Element types

Different type of 3D elements, shown in Table 3.2, have been offered by the nonlinear FE package, ABAQUS 6.13, to predict the behavior of RC structure. C3D20 and C3D8 are the most frequently used elements for modeling of concrete material. C3D20 element is a general purpose quadratic brick element with 27 (3x3x3) integration points whereas C3D8 element is simple linear continual solid brick element with 8 (2 x 2 x 2) integration points. In the present study, C3D8 element type has been employed for both solid elements (concrete and structural steel).

Table 3. 2. Various elements used in ABAQUS (ABAQUS,2014)

Element	Description	D.O.F.	Element shape
C3D8	Hexagonal Element	24	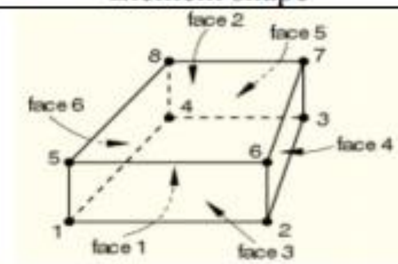
C3D20R	Hexagonal Element	60	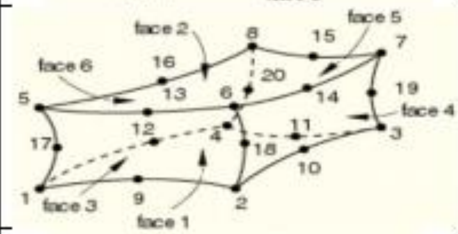
C3D4	Tetrahedral Element	12	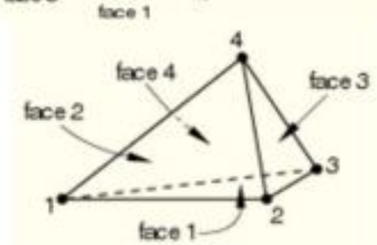
C3D10M	Tetrahedral Element	30	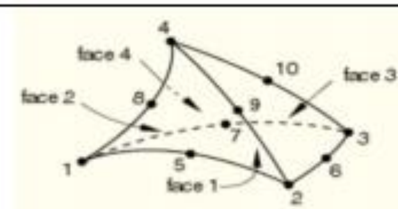

3.4.2. Concrete elements and constitutive relations

Modeling materials in computer programs is a challenge due to nonlinear propertis, and requires extensive data about the material's behavior. The concrete damaged plasticity model, which is a modification of the Drucker Prager strength hypothesis is a plasticity-based modl that arranges for the analysis of concrete structures under monotonic, cyclic and/or dynamic loading. Plasticity is characterized by the unrecoverable deformation when all loads are removed, and damage is defined by the decrease in elastic constants. Plasticity should be combined with damage to properly characterize the nonlinear behavior of concrete. Concrete behaves in a brittle way under low confining pressures and uniaxial compression (and tension). This behavior changes when the confining pressure is large enpugh to prevent crack propagation and when the concrete is subjected to multiaxial compressive stresses as shown in Figure 3.6. The material then becames more ductile and the compressive strength increase. The damaged plasticity model uses the yield funcrion of Lubliner et al., to represent different evoulution of strength under tension and compression. (ABAQUS, 2014).

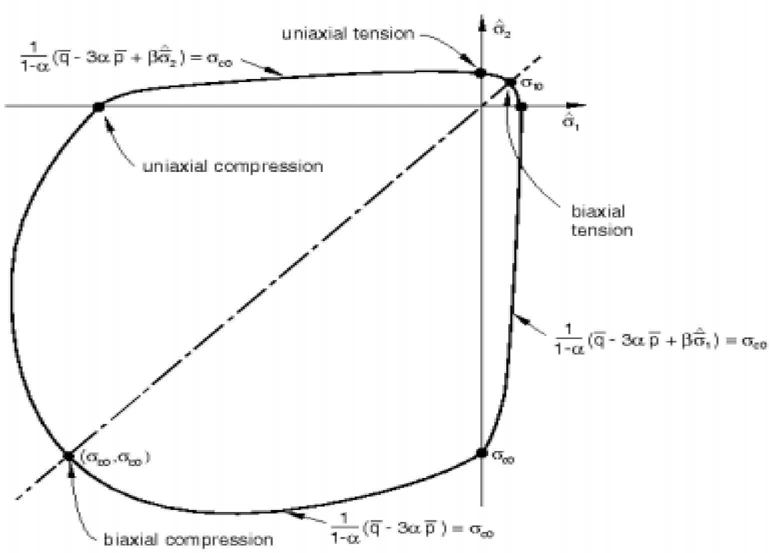

.

Figure 3. 6 Yield surface for plane-strain conditions at biaxial stress states (ABAQUS, 2014)

The inclination that the plastic potential reaches for high confining pressure is measured by dilation angle. It describes the behavior of concrete under multiples stresses. Small values leads to brittle behavior but greater values produce ductile behavior. The dilation angle should be chosen between 25^0 to 40^0 to describe both tension and compression in biaxial stress states for normal grade concrete. The default value in ABAQUS is 36^0.

Table 3. 3: Other default parameters of concrete damage plasticity model under compound stress

Parameter	**Denotation**
$\Psi = 36^o$	Dilation angle
f_{b0}/f_{c0}	Ratio of biaxial to uniaxial compressive strength
K =0.67	Second stress invarient ratio
e = 0.1	Eccentricity

The stress-strain curve of concrete is specified in Eurocode 2 section 3.1.5 (see Figure 3.7) and is made of a linear-elastic region until initial yield and plastic section (stress hardening followed by strain softening) is reached. (SS-EN 1992-1-1 (2005))

When no test results are available to determine the stress-strain curve for the concrete one can use the mean compressive strength f_{cm} to plot the curve. Other quantities needed in order to determin the points on the graph are (Yusuf Sumer, 2015)

$$E_{cm} = 22(0.1 f_{cm})^{0.3} \qquad (3\text{-}1)$$

$$\varepsilon_{c1} = 0.7(f_{cm})^{0.31} \qquad (3\text{-}2)$$

$\varepsilon_{cu} = 3.5\,{}^{o}\!/_{oo}$ Where

f_{cm} is in [MPa]

E_{cm} is the longitudinal modulus of Elasticity [GPa]

ε_{c1} is the strain at average compressive strength

ε_{cu} is the ultimate strain

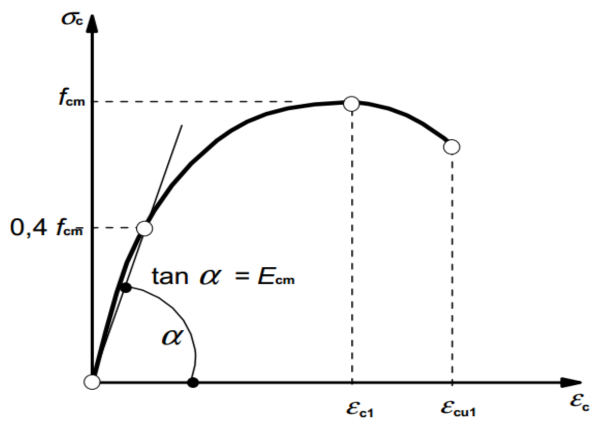

Figure 3. 7 Schematic representation of the stress-strain relation for structural analysis (Eurocode 2)

If the concrete grade is higher than C50/C60 the following formulas can be use

$$\varepsilon_{c1} = 0.0014\left[2 - \exp(-0.024 f_{cm}) - \exp(-0.140 f_{cm})\right] \quad (3\text{-}3)$$

$$\varepsilon_{cu} = 0.004 - 0.0011\left[1 - \exp(-0.0215 f_{cm})\right] \quad (3\text{-}4)$$

As shown in the above figure the stress-strain behavior of concrete in compression is assumed as linear elastic up to 0.4 f_{cm} .

$$\frac{\sigma_c}{f_{cm}} = \frac{k\eta - \eta^2}{1 + (k-2)\eta} \quad (3\text{-}5)$$

Where

$$\eta = \varepsilon_c / \varepsilon_{c1}$$

$$k = 1.05 E_{cm} \times \left|\varepsilon_{c1}\right| / f_{cm}$$

After plotting the graph, variables for compressive behavior can be obtained. Inelastic (crushing) strain $\varepsilon_c^{\ in}$ which occurs due to the opening of micro cracks merging to macro cracks, is determined by subtracting the elastic compressive part ε_{0c}^{el} from total strain ε_c (see figure 3.8). The inelastic strain is converted to plastic strain ε_c^{pl} by ABAQUS software. (ABAQUS, 2014)

$$\varepsilon_c^{in} = \varepsilon_c - \varepsilon_{oc}^{el} \quad (3\text{-}6)$$

$$\varepsilon_{0c}^{el} = \frac{\sigma c}{E_O} \quad (3.7)$$

$$\varepsilon_c^{\ pl} = \varepsilon_c^{in} - \left(\frac{dc}{1 - dc}\right)\left(\frac{\sigma c}{E_o}\right) \quad (3.8)$$

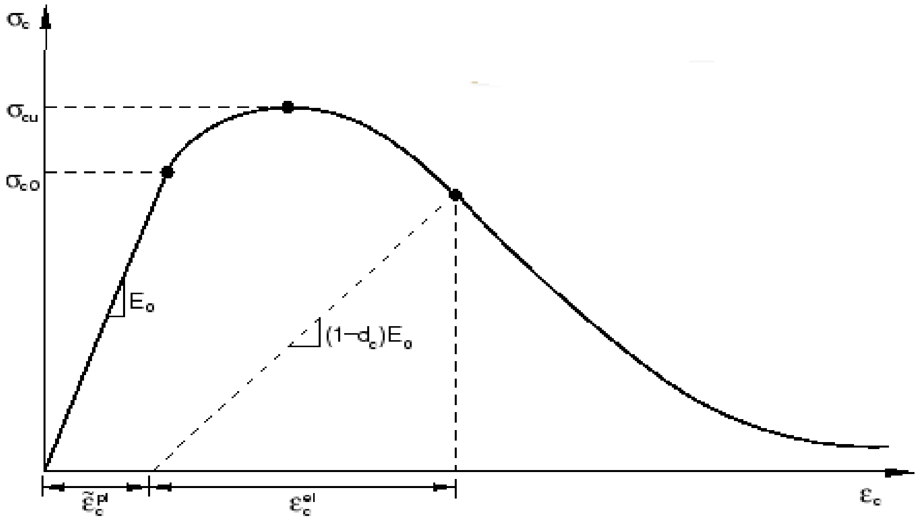

Figure 3. 8: Response of Concrete uniaxial loading in Compression

The post-failure behavior is simulated with tension stiffening by applying a fracture energy cracking criterion (see Figure 3.10). To determine the stress-strain curve for tension, a bilinear crack opening curve is used. (Yusuf Sumer, 2015)

$f_{ctm} = 0.3 f_{ck}^{(2/3)}$ for concrete grade $\leq$ C50 (3-9)

$f_{cm} = f_{ck} + 8$ (3-10)

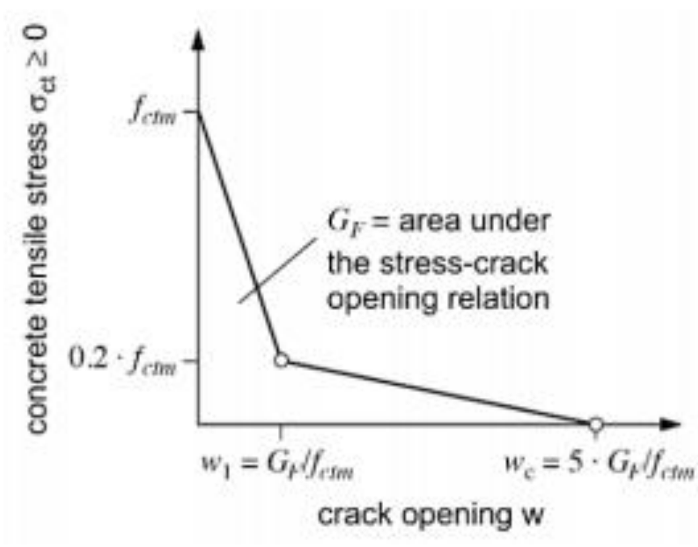

Figure 3. 9: Stress Crack Opening relation for uniaxial tension(ABAQUS,2014)

Figure 3.10 explains the cyclic response of concrete with the load transition phenomenon. Initially, the material behaves linearly up to the tensile failure stress σ_{t0}; representing the onset of micro-cracking in the concrete. Beyond this stress, the material propagates towards the strain softening mechanism of the cracked concrete. The failure behavior is defined by means of a post failure stress strain relation modeled by tension stiffening as the effect is more pronounced by tension side. This phenomenon also supports for the simple simulation of steel concrete interaction effects [ABAQUS, 2010]. During unloading and reloading, i.e. the transition of load from tension to compression, the elastic stiffness of concrete is damaged as the unloading response starts to weaken. The two damage variables, dt and dc ($0 \leq dt, dc \leq 1$) characterize the elastic stiffness degradation. The degradation mechanism gets complex under cyclic loadings, due to the opening and closing of previously formed cracks. As the load changes sign, the tensile cracks tend to close significantly which causes the material to recover some elastic stiffness named as stiffness recovery effect. This recovery generally characterizes the amount of the tension damage dt due to compressive loading. The reduction in the initial elastic stiffness E_0 is generally expressed by the following expression:

$$E=(1-d)\,E_0$$

The experimental observation in most quasi-brittle materials, including concrete, is that the compressive stiffness is recovered upon crack closure as the load changes from tension to compression. On the other hand, the tensile stiffness is not recovered as the load changes from compression to tension once crushing micro-cracks have developed. This behavior, which corresponds to $w_t = 0$ and $w_c = 1$, is the default used by ABAQUS. Figure 3.10 below illustrates a uniaxial load cycle assuming the default behavior.

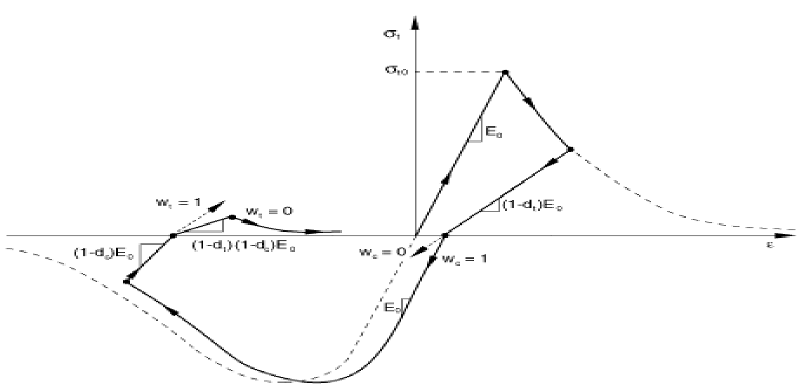

Figure 3. 10: Response of concrete under cyclic loading

In this study, behavior of mateials was defined and damage plasticity model of concrete was used including the damaged part. All parameters are derived from the only known parameter from the reference experiment: mean strength of the concrete f_{cm}. Young's modulus for concrete and data points of stress-strain curve was obtained based on the above equations. Density of concrete and poisson's ratio are based on the recommended values. For other parameters needed such as dilation angle, eccentricity, $f_{b0/f_{co}}$, k and viscosity parameter , ABAQUS's default data were used.

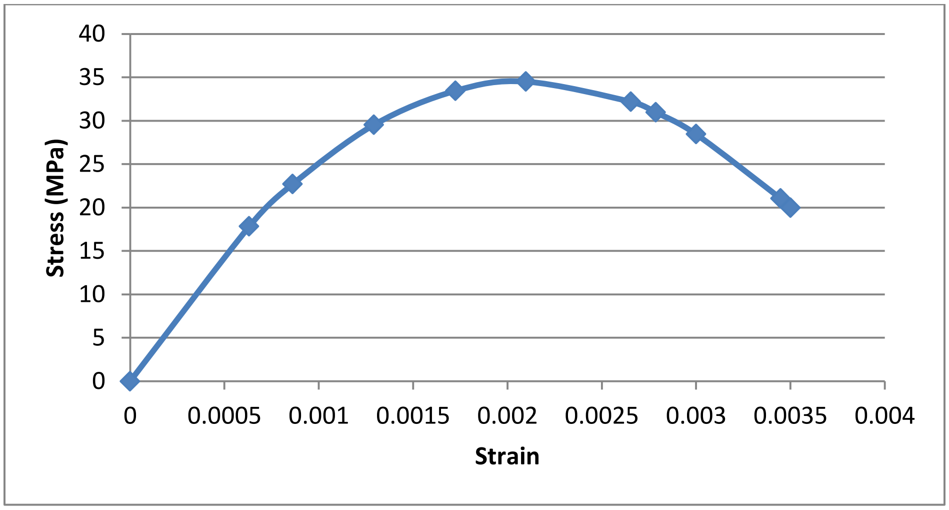

Figure 3. 11: Material curve for compressive behavior of the analysed concrete

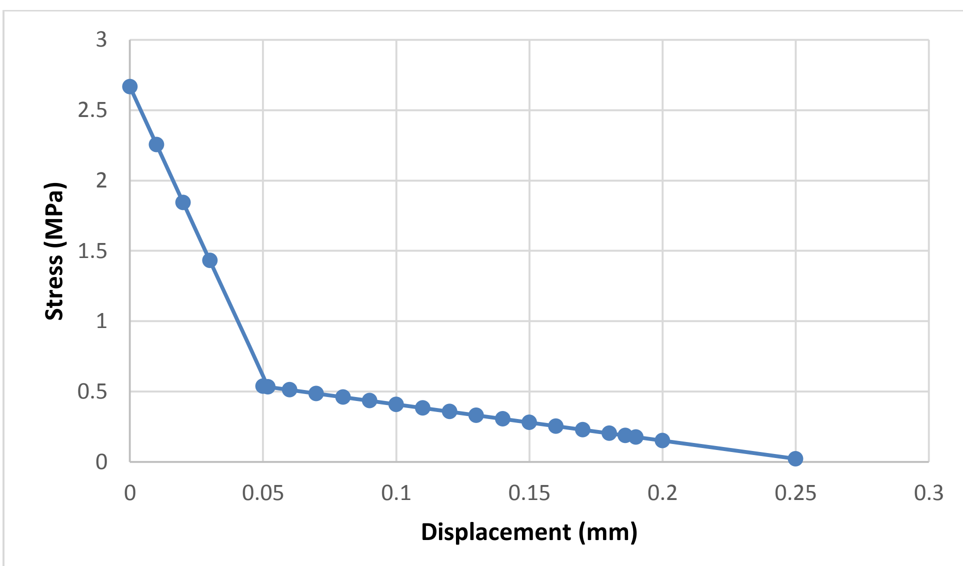

Figure 3. 12: Material Curve for Tensile behavior of the analysed concrete

Table 3. 4 Input material data for concrete

Density	2400kg/m^3
Young's modulus	31.8GPa
Poisson's ratio	0.2
Dilation angle	36
Eccentricity	0.1
f_{b0}/f_{c0}	1.16
k	0.667
Viscosity parameter	0

3.4.3. Steel Section and Reinforcement Bars

The structural steel section and the reinforcement bars are modeled as an elastic–plastic material in both tension and compression.The stress–strain responses in compression and tension are assumed to be the same. This response exhibits a linear elastic portion followed strain hardening stage until reach the ultimate stress. The metal plasticity model in ABAQUS was used to define the non-linear behavior of materials. The "ELASTIC" option was used to assign the value of 200× 10^3 N/mm^2 for the Young's modulus and 0.3 for the Poisson's ratio. The "PLASTIC" option also used to define the plastic part of the stress–strain curve. According to ABAQUS manual (ABAQUS, 2010), true stress and true strain should be used to define the non-linear behavior of material properties. So, the true stresses were assigned in ABAQUS as a function of the true plastic strain.

Mechanical properties for the steel section and reinforcement bars that are used in these simulations are given in Table 3.3

Table 3. 5. Mechanical properties of the steel section and reinforcement Bars

Part	Yield Stress (N/mm^2)	Ultimate stress N/mm^2)	Density (Kg/mm^3)	Young's modulus (kN/mm^2)	Poisson ratio
Steel Section	345	500	7850	200	0.3
Reinforcement Bars	413	600	7850	200	0.3

3.5. Geometric modeling and finite element mesh

The size of the finite element mesh has a significant effect on the results of the analysis of composite walls. The model with an unnecessarily fine mesh requires an extra amount of computation time while the model with a mesh that is too coarse might not be adequate to represent the behavior of the wall correctly. The proper size of the finite element mesh for reinforced concrete members depends greatly on the nature of the problem being studied. Because there are no definite rules for selecting the proper mesh size for the analysis of reinforced concrete members, testing of finite element models with different mesh sizes is usually a good way to gain an initial understanding about the proper mesh size and the sensitivity of the results to different mesh sizes in this study, the optimal mesh size has been found to be 100mm for concrete, structural steel and also for the reinforcement bars after so many trial runs.

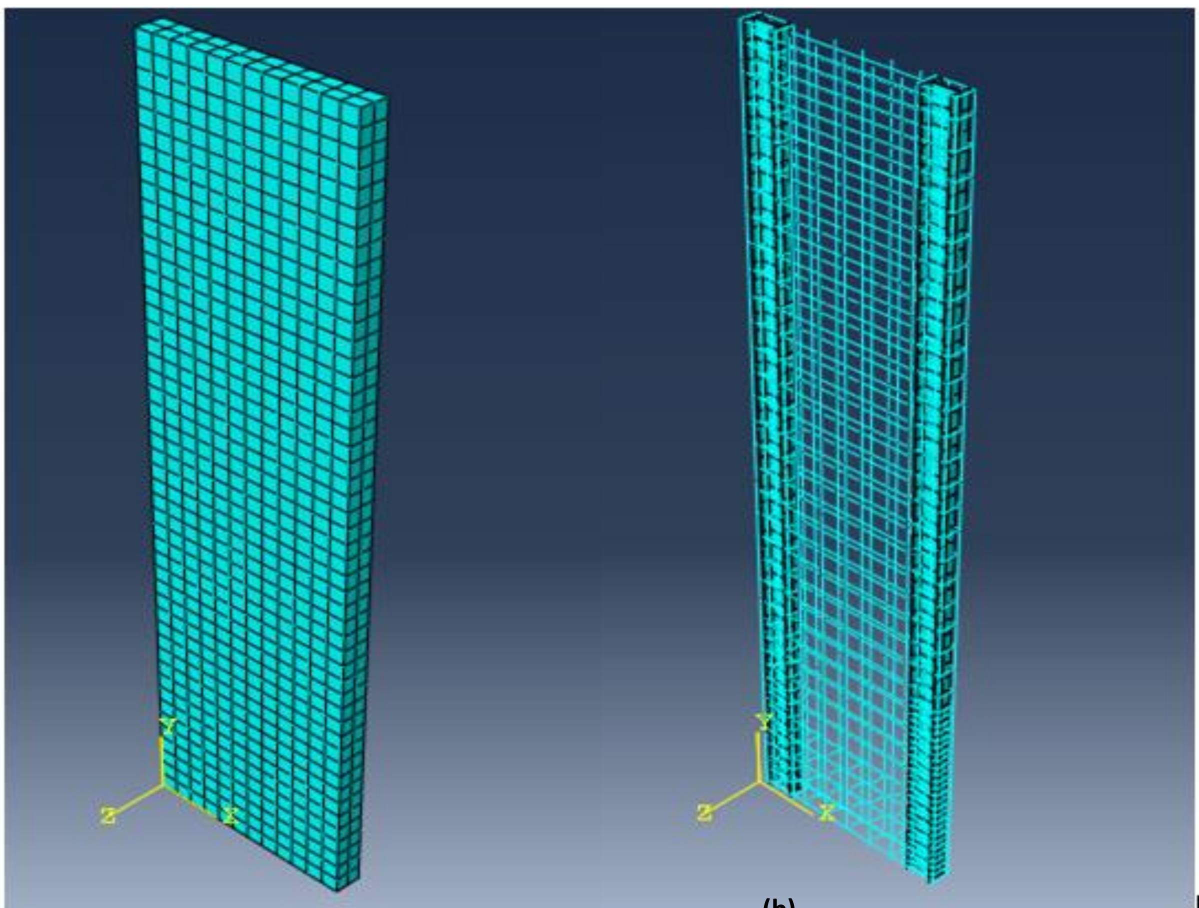

(a) (b)

Figure 3. 13: Finite Element mesh (a): Concrete mesh (b): Structural steel and reinforcement bars

3.6. Interaction

As the steel and concrete surfaces were directly adjoined in the test setup so the contact analysis procedure is developed in the FE model to simulate the experimental condition. The contact interaction option in ABAQUS is used in modelling the contact between steel and concrete in the composite shear wall by providing the geometric and mechanical properties for the interaction. First, the mechanical properties are specified and then associated with geometric features of the interaction to complete the contact assignment process. The mechanical property defined here, relates with the normal and tangential behaviour. The values were assigned as default which gives rise to relatively rigid contact condition.

The structural steel and the reinforcement bars of the shear wall are modelled as embedded regions in the concrete by using 'embedded constraint' option in the interaction module to account their contribution on the deformation capacity.

3.7. Boundary conditions and loading conditions

The numerical model under observation is fixed at the bottom to restrain each component of the shear wall in all degrees of freedom and to reflect the characteristics of the shear wall used for the experimental study. Load is simulated by applying the displacement control scheme rather than direct loading to generate cyclic behavior of the composite steel-concrete shear wall. Cyclic lateral loading has been applied via static load protocol with imposed drift levels up to 4%. The jumps in the displacement are regulated by tabular 'amplitude' that reflects the story drifts, as shown in Figure 3.15..

Constant axial load is applied at the top face of the wall as a pressure force and kept constant throughout the analysis. A reference point has been created and coupled with the top face of the specimen to apply the lateral load so that local failure will not be occurred (see Figure 3.14).

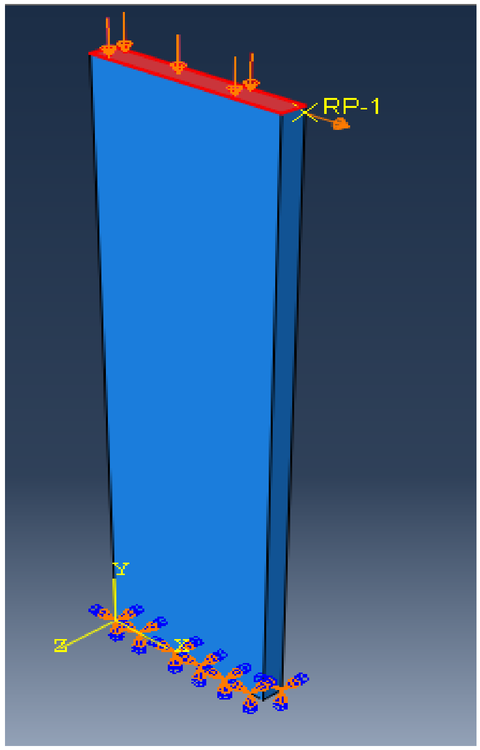

Figure 3. 14: Boundary and loading condition

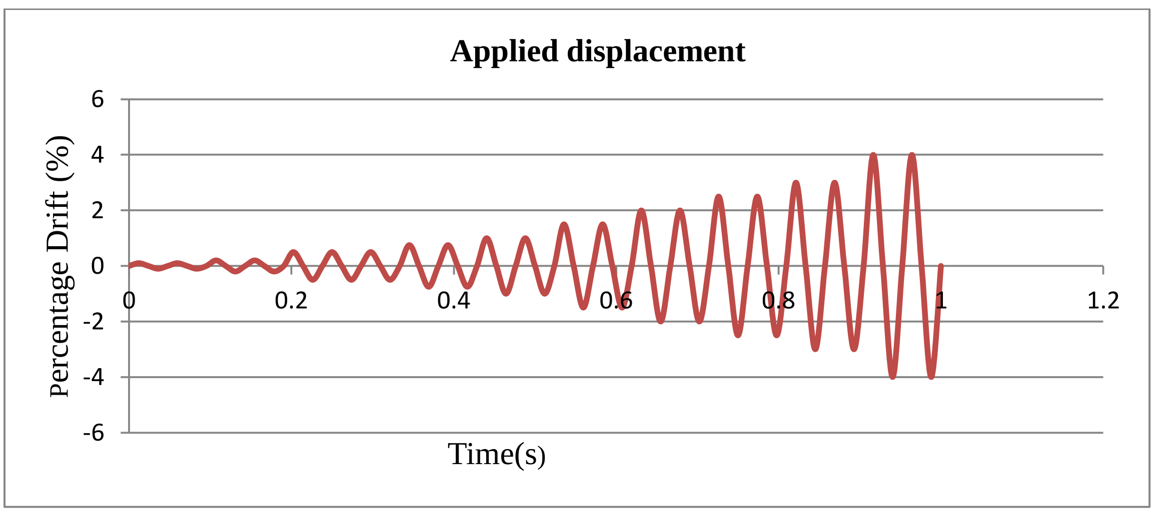

Figure 3. 15: Applied displacement Vs time

CHAPTER FOUR

PERFORMANCE EVALUATION OF FINITE ELEMENT MODEL AND PARAMETERIC STUDY

General

The finite element model developed in Chapter three is compared with the experimental result of the reference test specimen. The modeling is done to simulate the reference test specimen by trying different element types, material constitutive models, mesh sizes , interactions, amplitude and solution strategy. The result of the best combination model is used to compare the ultimate load and displacement of the simulation and experimental result.

4.1. Comparison of Expermental Result and FEM result

4.1.1 Cyclic Analysis

To capture the cyclic behavior of the experimental SRC walls, several cases have been tried in this study. Some of these are material model for steel and concrete, different loading rate (amplitude), boundary condition, mesh size and element type. The selected model captures the failure mode, the stress distribution and the lateral load capacity of the walls but can not capture the hysteresis loops perfectly. This seems like the material models integrated in ABQAUS modules have difficulties to capture the cyclic behavior of structural elements.

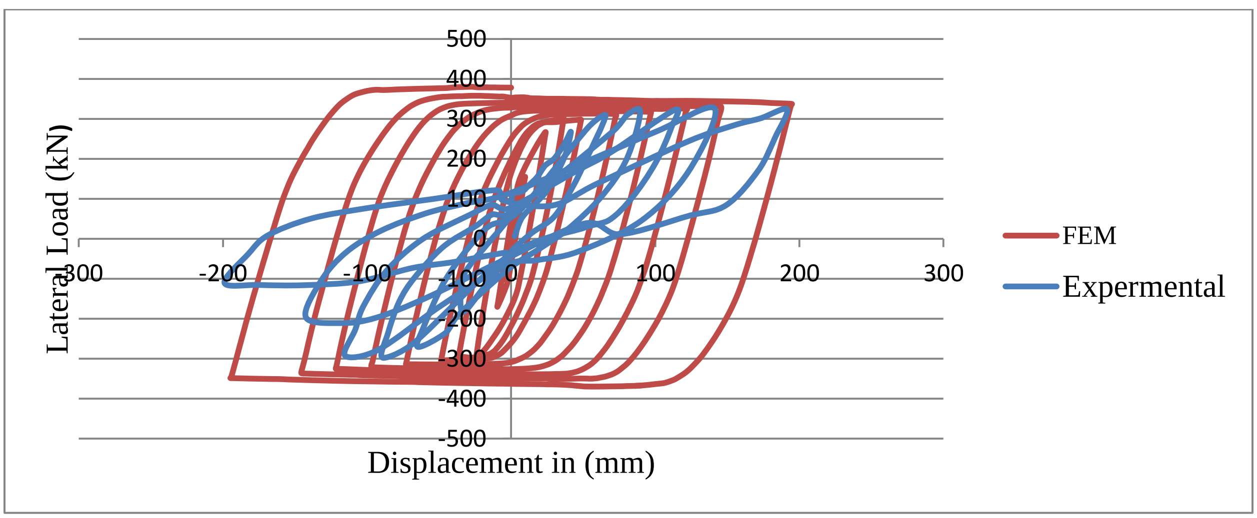

Figure 4. 1: Hysteresis curve of Expermental and FEM

4.1.1. Monotonic loading analysis

The Experimental result and ABAQUS result of top horizontal force versus horizontal displacement curve of the specimen is shown in Figure 4.2. The test result presented in Figure 4.2 shows the positive branch of the envelope of the cyclic alternating hysteretic load-displacement curve of the specimen, which cover only the first peak load values at the predetermined displacement levels. Comparing the numerical results with the experimental one, ABAQUS results show similar trends as that of test results and capture well the non-linear load-displacement response of the specimen. It indicates that the finite element analyses are capable of predicting the experimental behavior of the specimens when structural steel reinforced concrete shear walls are subjected to monotonic horizontal load.

Table 4. 1: Load capacity Expermental and FEM results

Specimen Desigination	Reinforcement		Experment peak load (kN)	FEM peak load (kN)	V_{exp}/V_{FEM}
	Boundary	Web			
SRCW1	8-12.7 A_s=1729	9.53@152	307	338.45	0.907
SRCW3	8-12.7 A_s=1729	9.53@152	337	370.5	0.91

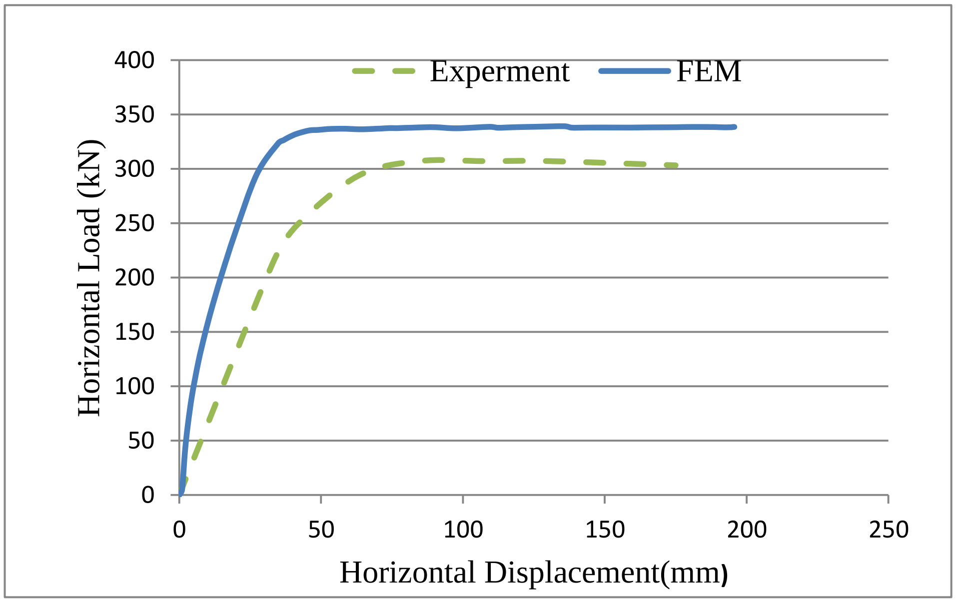

Figure 4. 2 : Monotonic finite element analysis compared with the envelope of test cyclic response (Lateral Load Vs Displacement) SRCW1

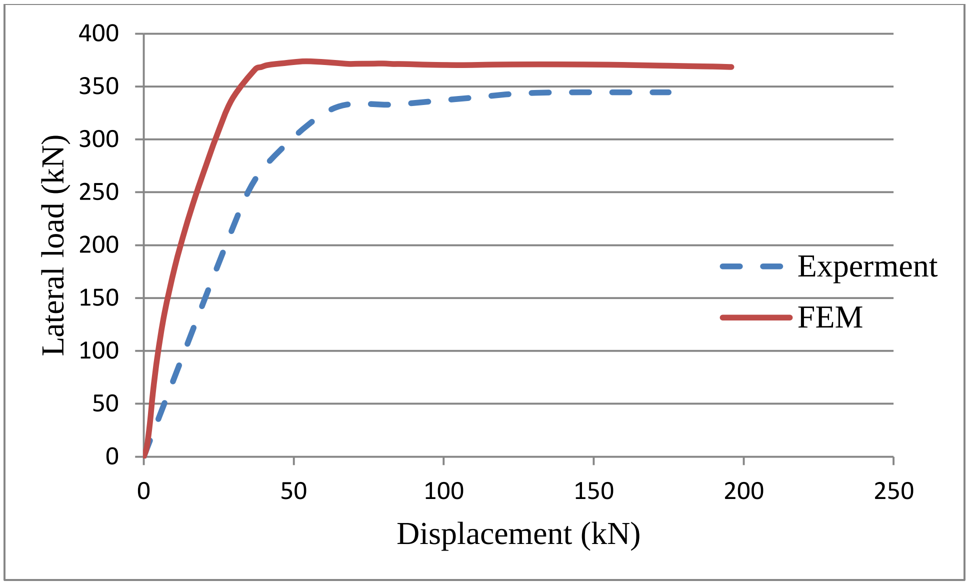

Figure 4. 3:- Monotonic finite element analysis compared with the envelope of test cyclic response (Lateral Load Vs Displacement) SRCW2

As shown in the above figures the responses from ABAQUS shear wall is stiffer than the tested one. One reason for this could be because material used to model the finite element model are perfectly homogenous, unlike those in actual structure. Moreover the boundary conditions are strictly defined in the finite element model and the discretization itself imposes additional constraints on the displacements. Additionally in the actual SRCW bond slip between the structural steels and concrete may lessen the stiffness of the actual structure.

Hysteresis loops and envelop of hysteresis curve were compared with the finite element result as shown in Figure 4.1. and 4.2. . Monotonic loading analysis provides a good estimate of the capacity of a structural steel reinforced concrete shear wall as it captures closely the envelope of cyclic response of wall

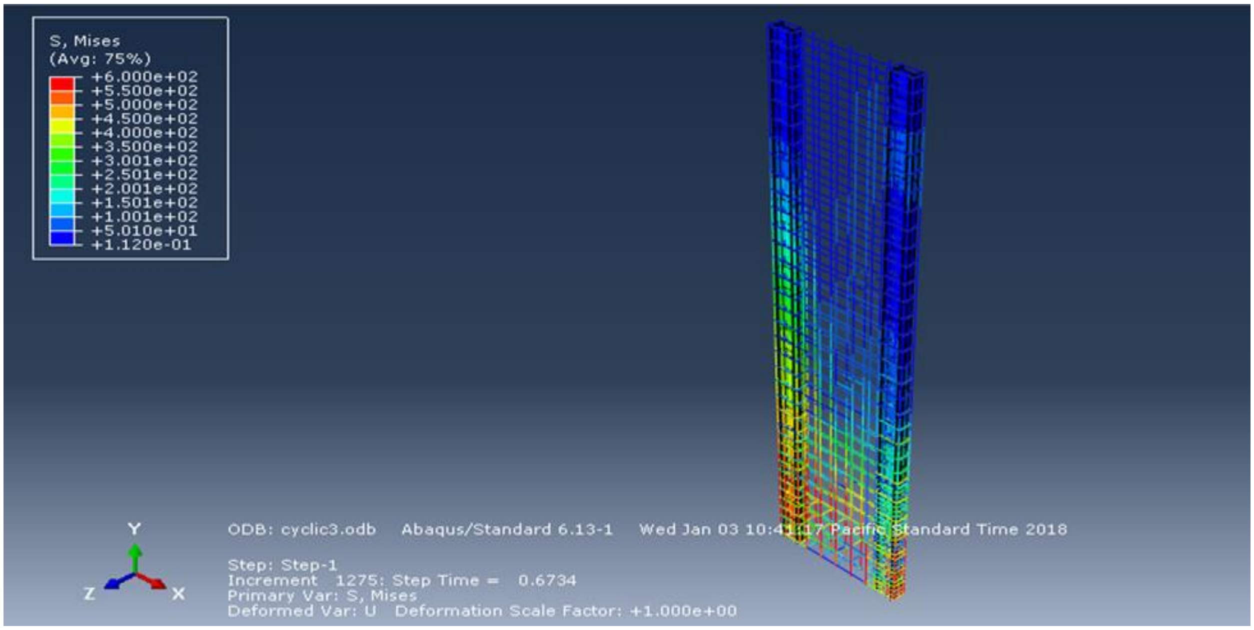

Figure 4. 4:- Stress distribution on the reinforcement and structural steel

As shown in Figure 4.3 the stress at the bottom steels reached ultimate stress which is equal to the input values given on Table 3.1 . This indicates that the reinforcement bars at the boundary are fully stressed and reached their ultimate capacity that there is a failure at those locations. In the experimental result also the reifocement bars at the boundary fractured at 4% drift level which is similar with the simulation failure mode.

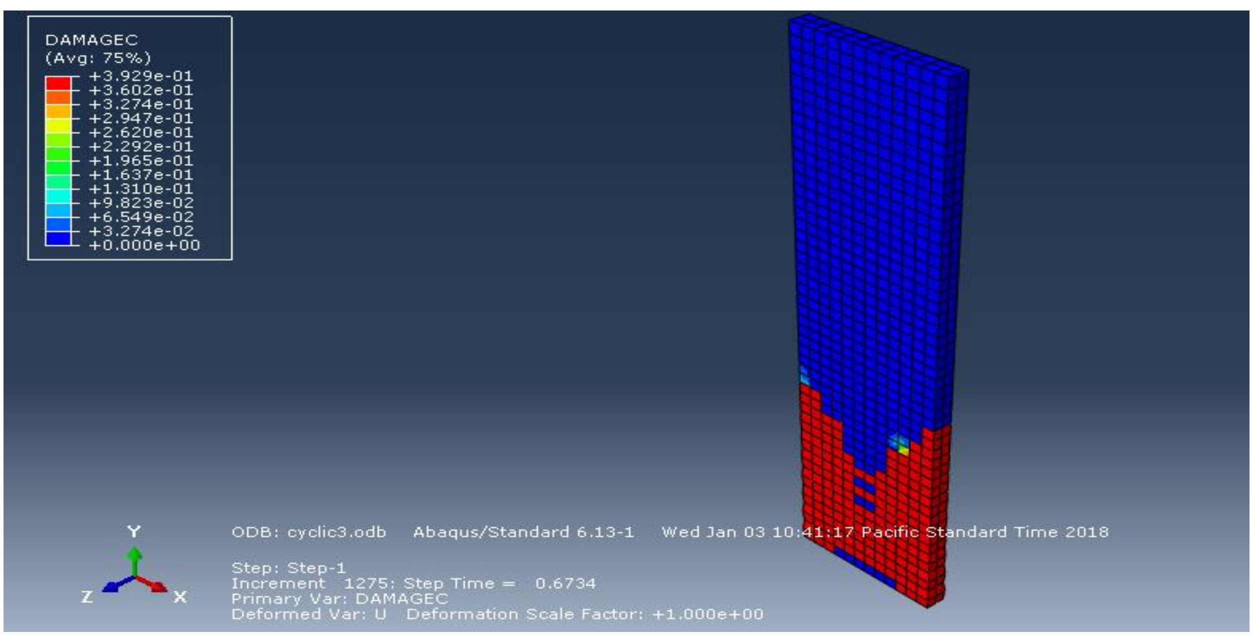

Figure 4. 5: Concrete Crushing

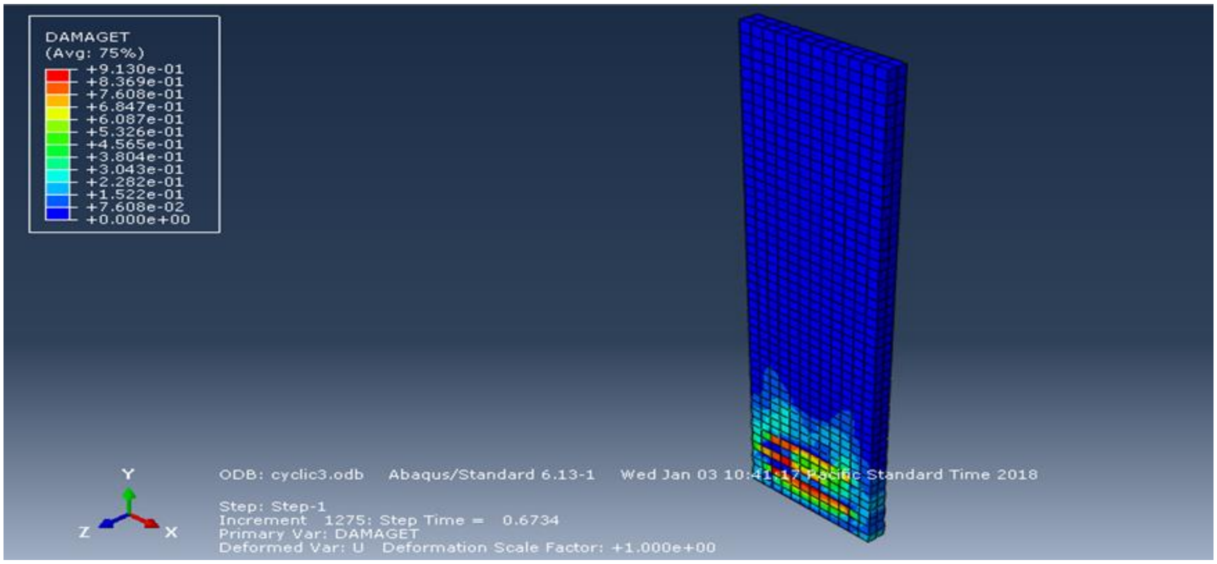

Figure 4. 6: Concrete Crack

As shown Figure 4.5. and 4.6. the concrete damage in compression and tension is up to its effective length which is 1220 mm of the wall, the contour indicate that concrete is fully damged at the bottom (it reaches the maximum damge parameter given in appendex A. which is inputed for this material). Comparing the pattern with the experimental result shows the simulation captures the failure mode perfectly.

4.2. Parametric study of Structural Steel Reinforced Concrete Walls

The finite element model developed in the previous chapter has been found to predict the behavior of structural steel reinforced concrete walls. This chapter presents a detailed case study on SRCW using the developed finite element model. The cases under study are cross sectional shape of structural steel at the boundary, axial load ratio , aspect ratio and concrete grade.

4.2.1. Effect of Cross sectional shape of structural steel used at the boundary

Different researches have been done to evaluate the performance of these walls under the conventional RC shear walls and found good results. However there is limited knowledge on the behavior of SRC walls with different types of structural steel and selecting the best shape .In this study four different shapes of structural steel at the boundary have been modeled and subjected under constant axial and cyclic lateral loading to investigate the load-deformation response, the failure mechanism and energy dissipation capacities of each walls.

The following abbreviations are used to identify the specimen afterwards. SRCWI (Structural steel reinforced concrete wall with I-section at the boundary), SRCWC (Structural steel reinforced concrete wall with Channel section at the boundary), SRCWR (Structural steel reinforced concrete wall with Rectangular hollow section at the boundary) SRCWT (Structural steel reinforced concrete wall with circular tube at the boundary)

The specimens have the same crossection with SRCW1 which is expermentaly tested one and the only difference between these four specimens is the shape of structural steel used at the boundary. The structural steel used at the boundaries have almost the same area in order to have the same nominal moment strength.

Table 4. 2: Description of specimens selected for analyzing the effect of structural steel shape at the boundary

Specimen Id	Shear wall dimension(H*L*t)(m)	Aspect Ratio	Shape of steel section at the boundary with their dimension (mm)	Ag of the steel section (mm^2)
SRCWI	4.8*1.2*0.152	4		1729
SRCWC	4.8*1.2*0.152	4	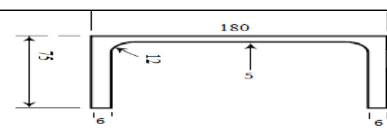	1750
SRCWR	4.8*1.2*0.152	4	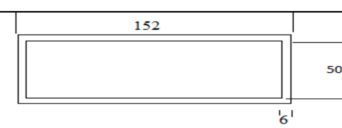	1711
SRCWT	4.8*1.2*0.152	4	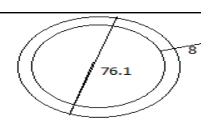	1716

4.2.2. Effect of axial load ratio

Reinforced concrete (RC) shear walls have been widely used as the major lateral force-resistant components in high-rise buildings because of their large lateral stiffness and strength. Shear walls usually withstand a considerable amount of axial compressive force exerted from gravity loads. The axial force level of shear walls is indicated by the axial force ratio n, which is calculated as $n = N/(A_g f_c)$ where N denotes the compressive axial force acting on the wall, Ag denotes the wall's gross cross-sectional area, and fc' denotes the compressive strength of concrete. Extensive studies have shown that RC walls under high axial force ratios have low ductility and limited deformation capacity when subjected to cyclic lateral loads in this study the effect of axial force level has been investigated on structural steel reinforced concrete wall for different aspect ratio. The lateral load carrying capacity and failure mode has been studied.

For investigating the effect of axial ratio Structural steel reinforced wall with hollow rectangular section at the boundary have been selected and designed based on the procedure of design of ductile walls.

4.2.3. Effect of Aspect ratios

In order to study the effect of wall aspect ratio (h/lw) on strength of wall, 7 cases have been considered in the analysis .Aspect ratio (h/lw) of 1,1.5,2,2.5,3,3.5 and 4 has been pushed up to 4% drift . All the walls are similar with the SRC walls , the only difference between these wall is their height .

4.2.4. Effect of Concrete Grade

In order to investigate the effect of concrete grade on the behavior of SRC walls 6 spaciments have been selected which are the same with SRCWI with all parameters but different with concrete grade only. C40,C50,C60 and C70 are the selected grade of concrete for this analysis.

4.2.5. Sensitivity Analysis

Five parameters have been selected in order to show the influence of the parameters on the strength of shear wall. The input parameters for sensitivity analysis are geometrical characteristics and strength characteristics of the test specimens where as probabilistic and stastical quatities were obtained from Latin Hypercube Sampling Technque (LHST) for the given mean value and standard diviation.

Table 4. 3: Mean values and standard deviation of geometric and strength characteristics

	Parameter		Mean μ_i	Std σ_i
1	Thicness of wall t_w	mm	170	8.5
2	Flange thickness of channel section t_f	mm	8	0.4
3	Structural steel yield strength f_{ys}	MPa	345	17.25
4	Reinforcement bar Yield strength f_y	MPa	413	25.15
5	Concrete strength f_c	MPa	40	2

The model is done for the same specimen with SRCWC (channel section at the boundary) by remodeling according to the combination below found from Latin hypercube sampling technique for the above inputs. The model combinations studied are tabulated in Table 4.4 below.

Table 4. 4:- Latin hypercube sampling technique software result for the given mean and standard diviation values

Comb	t_w	t_f	f_{ys}	f_{ybar}	f_c
comb1	192.87	7.42	326.41	380.41	39.61
comb2	167.13	8.50	320.54	418.22	42.46
comb3	165.32	8.76	316.09	450.57	41.66
comb4	183.06	8.98	361.33	390.99	40.89
comb5	163.30	7.24	340.21	393.80	37.84
comb6	189.70	7.97	332.50	416.12	37.54
comb7	181.83	7.14	354.20	438.09	39.11
comb8	160.94	7.84	351.21	429.59	39.28
comb9	170.30	8.16	345.68	432.20	39.44
comb10	191.23	9.72	342.97	401.20	36.65
comb11	174.42	7.34	307.85	375.43	39.76
comb12	178.17	7.78	341.60	396.41	38.55
comb13	179.39	9.34	373.91	445.59	44.31
comb14	213.39	7.91	369.46	368.59	42.84

Comb	t_w	t_f	f_{ys}	f_{ybar}	f_c
comb15	146.61	8.86	337.32	409.88	43.35
comb16	185.58	7.57	347.03	384.45	40.24
comb17	196.70	8.22	323.78	411.96	40.72
comb18	168.77	8.03	335.80	414.04	38.75
comb19	154.02	6.87	330.67	424.80	41.07
comb20	173.10	8.58	352.68	470.08	41.25
comb21	184.30	8.29	357.50	355.92	39.92
comb22	186.90	7.50	328.67	427.14	40.39
comb23	175.70	8.09	359.33	422.54	40.56
comb24	180.61	8.36	348.40	398.86	38.34
comb25	158.02	6.66	366.22	403.46	42.16
comb26	176.94	7.71	363.59	387.91	40.08
comb27	194.68	8.43	338.79	441.55	38.93
comb28	199.06	8.66	355.80	420.36	37.16
comb29	201.98	7.02	344.32	435.01	35.69
comb30	205.98	9.13	382.15	405.64	41.89
comb31	188.27	7.64	334.20	457.41	38.11
comb32	171.73	6.28	349.79	407.78	41.45

CHAPTER FIVE

RESULT AND DISCUSSION

From the analysis in the previous chapter, it can be concluded that the finite element analysis developed in this study can well simulate the load carrying capacity of SRC walls so that it is possible to continue the study to study the effects of structural steel shape, axial load ratio, aspect ratio and concrete grade on the behavior of these walls. The results will be discussed in this section.

5.1. Effect of structural steel shape used at the boundary

All four specimens are modeled with the same element, mesh size, boundary condition and also same loading condition which is a displacement controlled loading conditons pushed up to 4% drift to compare the load displacement of the specimens.

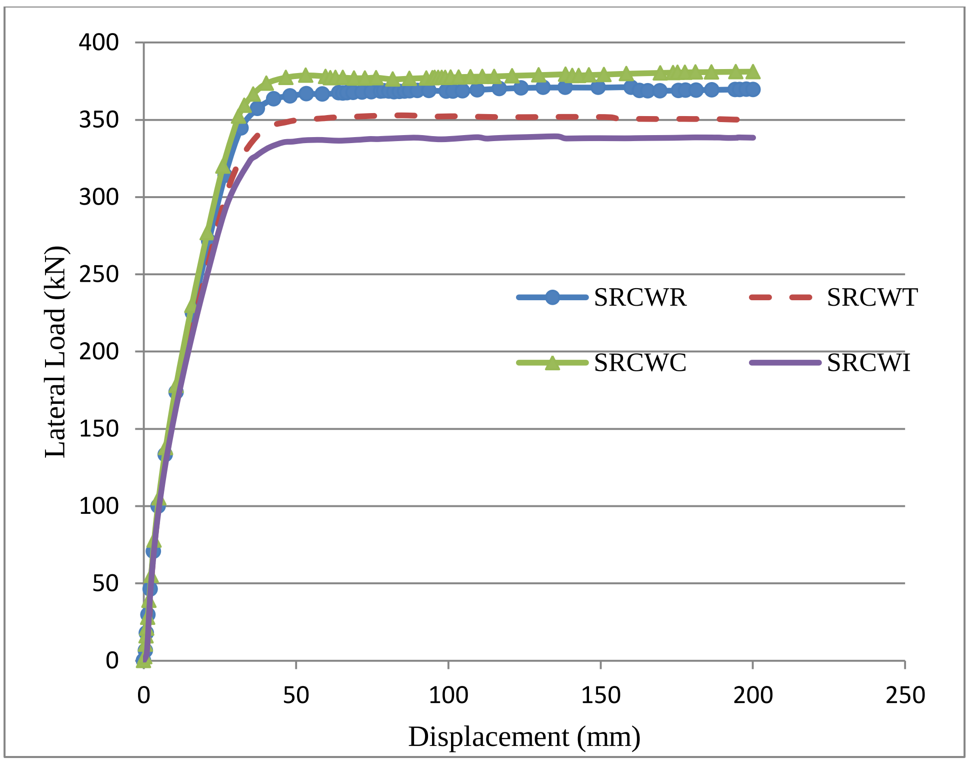

:

Figure 5. 1:load versus displacement for shear wall with different shape of structural steel at the boundary

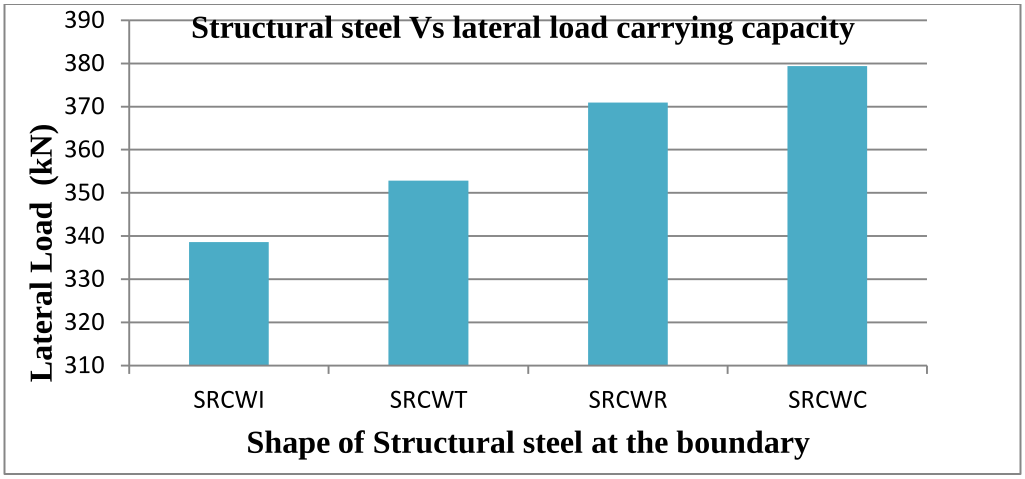

Figure 5. 2: Structural Steel shape used at the boundary Vs Load Carrying Capacity

All specimens have similar load deflection response as shown in Figure 5.1 but there is some variation on their load carrying capacity especially between SRCWI and SRCWC (which is 10.6% variation on load carrying capacity). SRCWC resists a larger amount. This may be due to the moment of inertia of the structural steel cross section. SRCWI and SRCWT vary with 14kN which means 3.9% and SRCWI and SRCWR with 34kN which is a percentage of 9.14%.

For SRCWI and SRCWC specimens the capacity is increasing up to 4% drift but on SRCWR the load starts to decrease at a displacement of 160.083mm and on SRCWT the decrease in load strats at a displacement of 110.675mm.

5.2. Effect of axial load on the behavior of shear wall

Seven shear wall which are the same with SRCWI with cross section, concrete, reinforcement ratio have been loaded for different axial load ratio to see the influence of axial load on the load carrying and ductility of SRC walls.

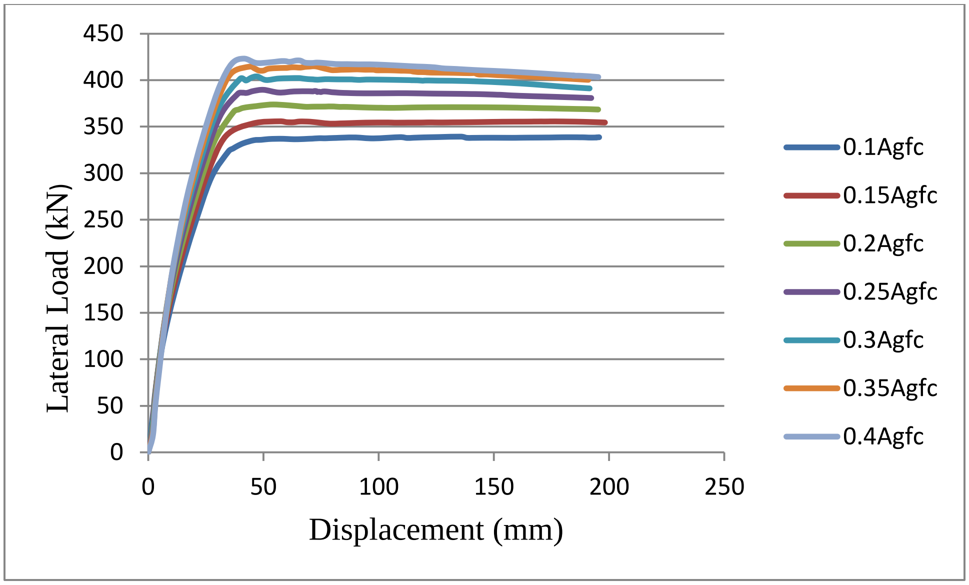

Figure 5. 3: Load Vs Displacement for different Axial Load Ratio

As shown in Figure 5.3 above an increase in axial load increases the load carrying capacity especially for the axial load ratio up to o.3Agfc' but above 0..3 the capacity became almost constant or the increase became very small. The increase in load carrying capacity, the displacement, ductility at yield and ultimate loads are shown in the Table 5.1 below

Table 5. 1: Summary of load and deflection at yield and ultimate for different axial load ratio

Axial Load Ratio	Yield Load (kN) Py	Deflection at Yield load (mm)Δ_y	Ultimate Load (kN) P_u	Deflection at Ultimate load (mm) Δ_u	Ductility index $(\frac{\Delta_u}{\Delta_y})$	Load carrying capacity increase with 0.05 axial load ratio variation(%)
0.1	122.67	6.7501	338.3814	195.696	28.9	
0.15	140.36	7.895	352.8774	195.54	24.76	4.28
0.2	179.35	10.036	369.7578	171.793	17.1	4.18
0.25	190.98719	12.087	385.0418	153.458	12.69	4.13
0.3	210.674	13.067	399.1815	134.884	10.25	3.6
0.35	22.365	14.212	410.023	110.927	7.8	2.6
0.4	240.673	15.647	412.755	66.1173	4.22	0.6

From the anlyis, it can be concluded that higher axial compression tends to increase the shear strength of SRC walls. This is because axial compression not only can enhance the shear strength of walls, but also the moment resistance in some cases (Wallace et al., 2012). Nevertheless, the enhanced shear strength attributed to axial compression generally cannot compensate for the adverse effect of reduced drift capacity, as after all, the system ductility is far more important than the strength in seismic design.

5.3. Effect of Aspect Ratio on the capacity of SRC walls

Five shear walls with different aspect ratio of 0.5, 1, 1.5, 2, 2.5, 3 ,3.5 and 4 are modelled in ABAQUS 6.13. All five shear walls have the same reinforcements, the same boundary cross section, the same web thickness and the same concrete strength as those parameters in SRCWI., so as to clearly see the effect of the only variable, aspect ratio, on the load resistance of Structural Steel Reinforced concrete walls. The load versus displacement curve is shown in Figure 5.4 below.

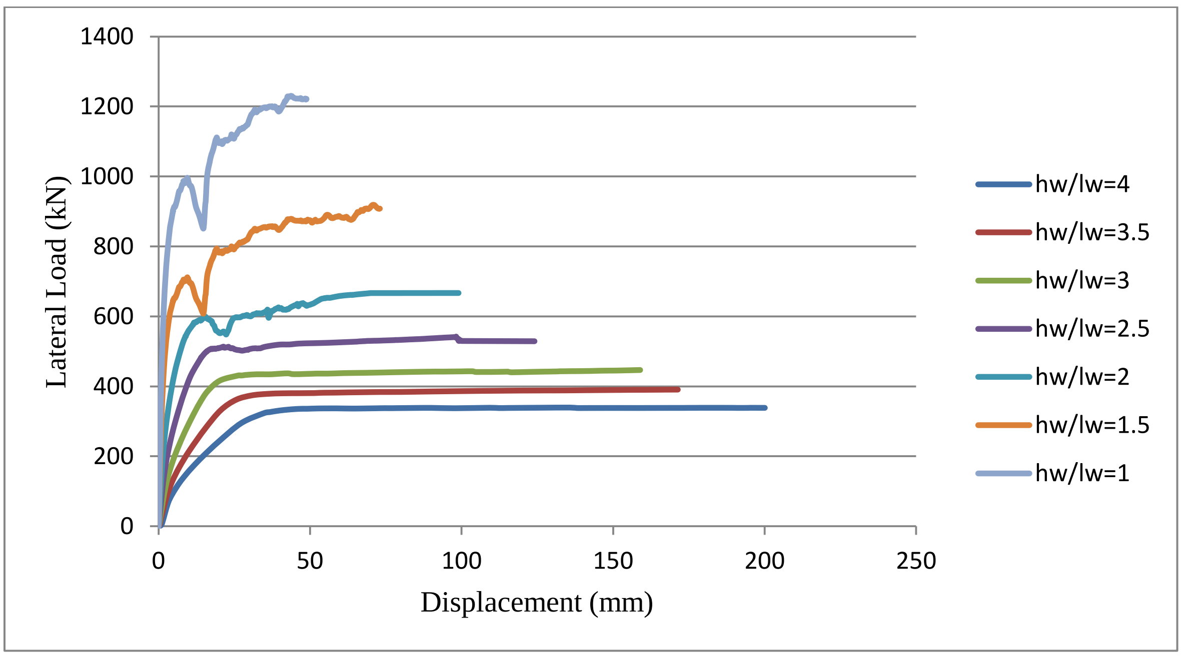

Figure 5. 4: : Load Vs Displacement curves for different aspect ratio of wall

To clearly visualize the relationship between aspect ratio and load carrying capacity, aspect ratio Vs lateral load has been presented in Figure 5.5

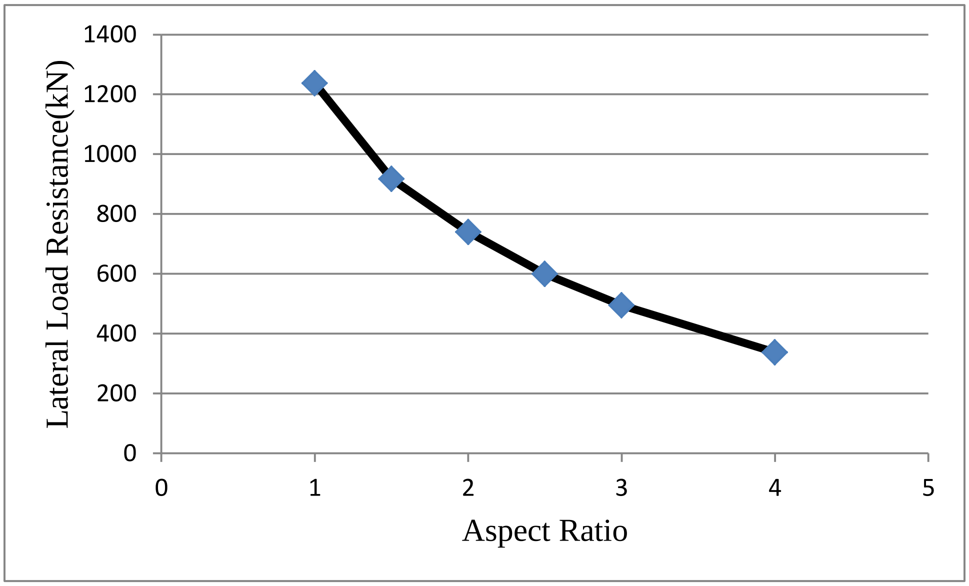

Figure 5. 5: Aspect Ratio Vs Lateral Load Resistance

As shown in the above figures aspect ratio plays important role in providing stiffness and strength to the wall. When height is equal to length of wall, i.e., aspect ratio is 1; under lateral load strut action can be observed and shear is predominant. Load carrying capacity is high as shown. For Aspect ratio 2, on the other hand,under lateral load strut action can not happen due to more height but shear is still predominant. Strength of the wall is reduced to 60 % when compared to aspect ratio 1. So for increase in aspect ratio from 1 to 2, strength is reduced by 40%. For Aspect ratio 3 due to high aspect ratio wall is predominant in bending. Its strength is reduced by 40% compared with aspect ratio 1. So when aspect ratio is increased by 3 times strength is reduced by 60%. For Aspect ratio 4, it is also predominant in bending as the case above. Its strength is reduded by 30% compared with aspect ratio 1. So when aspect ratio is increased by 4 times strength is reduced by 70%.

From this analysis it can be concluded that with the increase of aspect ratio the load carrying capacity of SRC wall reduced. The relationship between aspect ratio and lateral load resistance is inversely related and the it behaves approximately an inclined line.

5.4. Effect of concrete grade on the capacity of SRC walls

Figure 5.6. below provides the results of load carrying capacity for SRC walls. The walls are the same with SRCWI and the only difference between these walls is the concrete compressive strength which varies from 34.5 MPa to 60MPa. It indicates that concrete compressive strength has obvious effect on the load carrying capacity of shear wall. With the increase of concrete compressive strength, the lateral load carrying capacity of walls increases.

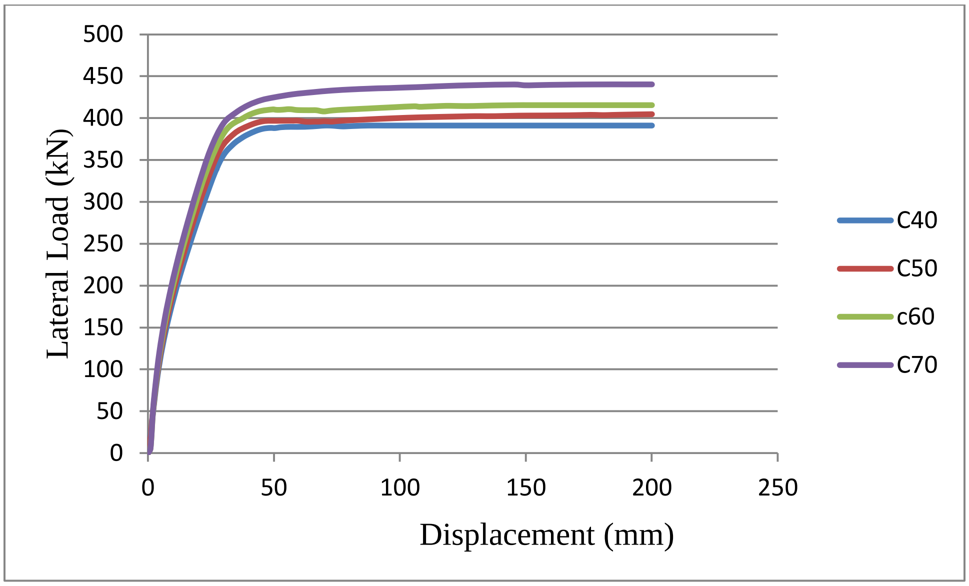

Figure 5. 6: Load Vs Displacement for different concrete grade

From the figure it can be seen that the load displacement curve have the same pattern for different concrete grade.

5.5. Sensitivity Analysis

Using the input parameters, 32 combinations were modeled in ABAQUS and their lateral load capacity have been taken. Regression have been done to relate the input parameters.

Table 5. 2:- simulation result of different combination with their capacity

Comb	V_c	Comb	Vc	Comb	Vc	Comb	Vc
comb1	442.329	comb9	454	comb17	448.284	comb25	437.802
comb2	424.836	comb10	507.269	comb18	446.337	comb26	467.328
comb3	467.939	comb11	393.14	comb19	427.249	comb27	468.539
comb4	502.809	comb12	448.51	comb20	500.248	comb28	489.004
comb5	398.832	comb13	517.45	comb21	455.64	comb29	452.553
comb6	448.214	comb14	488.983	comb22	433.984	comb30	453.358
comb7	502.809	comb15	439.088	comb23	459.028	comb31	455.944
comb8	463.362	comb16	417.405	comb24	472.536	comb32	536.754

Correlation coefficients are calculated between all random input variables and response variable (capacity of shear wall). These coefficients show the relative influence of random variables on value of capacity of shear wall; the correlation coefficient is higher, the resistance is more dependent on the parameter. A positive coefficient represents a direct dependence and if the correlation is negative, capacity is inversely proportional to the parameter. In this study all the parameters selected have a direct relationship with the capacity that means the correlation coefficients are positive. Regression has been done and the following equation is developed to determine the capacity of shear wall.

Table 5. 3: Correlation Coefficients

Parameter	Correlation coefficient
t_w	0.377
t_f	5.623
f_{ys}	0.903
f_{yb}	0.413
f_c	0.583
Intercept	-158.065

$$V_c = fn(t_w, t_f, f_{ys}, f_{yb}, f_c)$$

$$Vc = 0.377t_w + 5.623t_f + 0.903f_{ys} + 0.413f_{yb} + 0.583f_c - 158.218$$

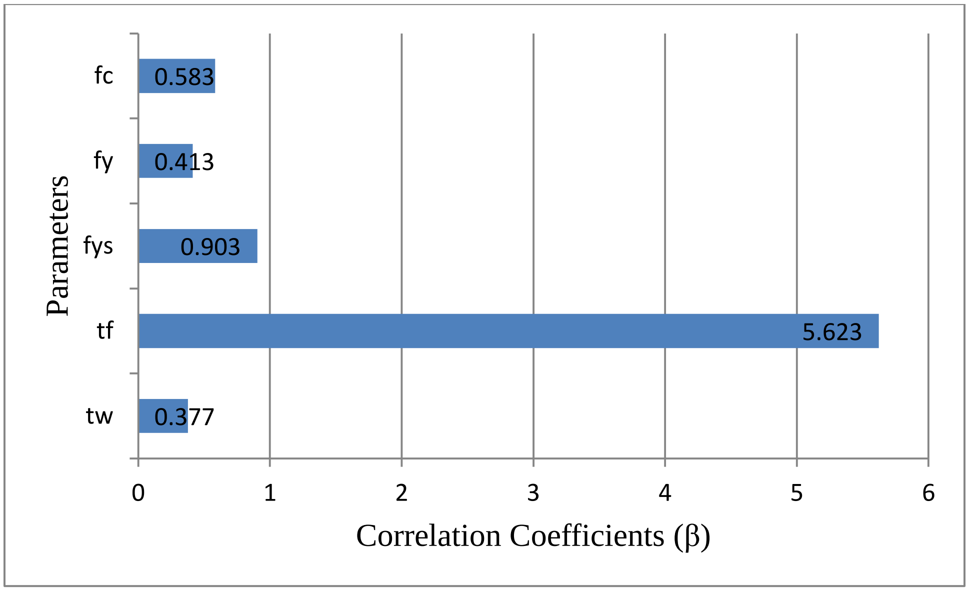

Figure 5. 7: Graphical Representation of correlation coefficients

As shown in Figure 5.7 for the geometrical parameters the influence of thickness of flange of structural steel is much greater that the thickness of wall in the capacity of shear wall . For the material strength, yield strength of structural steel has a higher influence almost twice greater than concrete grade and more than two times yield strength of reinforcement bar.

CHAPTER SIX

CONCLUSIONS AND RECOMMENDATIONS

6.1. Conclusions

In this study,Structural Steel Reinfoced Concrete Shear wall subjected to axial and cyclic loading was analyzed. As mentioned in detail in the previous sections, an experimental research on Structural Steel Reinforced Concrete Shear wall was selected as a base specimen. Finite element model was made and calibrated considering the report of experimental results. The calibrated model was used to conduct different case studies.

- ABAQUS 6.13 able to simulate the behavior of SRC walls under monotonic loading but have difficulty for simulating the hysteresis behavior of SRC structures.
- Study on the effect of structural steel shape used at the boundary shows SRCWC, SRCWR and SRCWT have a larger load carrying capacity than the base specimen SRCWI by 10.9 % , 9.14% and 3.9 %, respectively.
- Axial load ratio has an effect on strength and ductility of wall. From 10% to 15%, 15 to 20% , 20% to 25% , 25 to 30%, 30% to 35% and 35 to 40% of $f_c'A_g$ of axial load the percentage increase in load carrying capacity is 4.28,4.18,4.13,3.6,2.6 and 0.6 respectively. Regarding the ductility for 5% variation in axial load ratio the ductility index decreases 15%, 30.9%, 31.8%, 32.2% 23.9% and 45.8% .
- Aspect ratio plays important role in providing stiffness and strength to the wall. When height is equal to length of wall i.e aspect ratio is 1; Load carrying capacity is 40% larger than wall with aspect ratio 2 and shear is predominant in both cases. So for increase in aspect ratio from 1 to 2; strength is reduced by 40%. For Aspect ratio 3, due to high aspect ratio wall is predominant in bending. Its strength is reduced by 40% compared with aspect ratio 1. So when aspect ratio is increased by 3 times strength is reduced by 60%. For Aspect ratio 4, it is also predominant in bending as the case above. Its strength is reduded by 30% compared with aspect ratio 1. So when aspect ratio is increased by 4 times strength is reduced by 70%.
- As expected concrete grade has an impact on the strength of SRC walls. For walls pushed up to 4% drift the capacity of the wall increases as concrete grade increases.

- Finally sensitiveity analysis are presented, the aim of sensitivity analysis was to find out which input parameters has the greatest influence of the resistance of structural steel reinforced concrete walls. 32 models have been analysed differing in thickness of wall, thickness of flange of structural steel, yield strength of structural steel, yield strength of reinforcement bar and grade of concrete. It is found from the results of sensitivity analysis that for the geometric parameter thickness of flange has a greatest influence on the capacity. For the material strength, yield strength of structural steel has a higher influence almost twice greater than concrete grade and more than two times yield strength of reinforcement bar.

6.2. Recommendations

- The most important thing on earth quake resisting structures is the ductility of structural members not load carring capacity of a member so from this study it can be recommended that shear walls with higher axial load which is greater than 0.3Agfc should be avoided because the higher axial load ratio the lesser ductility.
- To study the seismic behavior of SRC walls , further investigation should be conducted by integrating a user defined material which capture the cyclic behavior in ABAQUS to see the true hysteresis behavior of SRC walls.

References

ABAQUS. (2014). *ABAQUS Documentation.* Providence,RI, USA: Dassault Systems.

ACI. (2014). *Building Cod Requirements for Structural Concrete(ACI 318-14).* America: American Concrete Institute.

Ahmed Ali, D. K. (2013). Modeling Of Nonlinear Cyclic Load Behavior Of I Shaped Composite Steel-Concrete Shear Walls Of Nuclear Power Plants. *Nuclear Engineering And Technology*, 89-98.

AL-Bdoor, M. (2013). *Behavior of composite columun subjected to Lateral Cyclic Loading.* Gazimagusa: Eastern Mediterian University.

B.Alfarah, F.-A. (2014.). New methodology for calculating damage variables evolution in plastic damage model for RC structures.

D Dan, A. F. (2011). Theoretical and expermental study on composite steel-concrete shear walls with vertical steel encased profiles. *Elsevier*, 880-813.

Daniel Dan, V. S. (2009). *Numerical Analysis of Composite steel Concrete Structural shear Walls with Steel Encased Profiles.* Universitatea Technica,, Gheorghe Asachi" din Iasi.

Enginers, A. S. (2000). *Prestandard and Commentary for the Sesmic Rehabitation of Buildings* . Washington, D.C.: Federal Emergency Management Agency.

Eurocode,2(2004). EN 1992-1-1:Eurocode 2 :Design of concrete structures-part 1-1: General rules and rules for buildings. London: British Standard Institution

FEi-Yu Lio, L.-H. h. (2012). Performance of reinforced concrete shear walls with steel reinforced concrete boundary columns. *Elsevier*, 186-209.

Feo-Yu Liao, L.-H. H. (2012). Performance of reinforced concrete shear walls with steel reinforced concrete boundary columns. *Elsevier*, 186-209.

Hong-Song Hu, J.-G. N.-S.-X.-H.-Y. (2016). Sesmic behavior of CFST-enahanced steel plate-reinforced concrete shear walls . *Constructional Steel Research*, 176-189.

Jiaru Qian, Z. j. (2012). Behavior of steel tube-reinforced concrete composite walls subjected to axial force and cyclic loading. *ELSEVIER*, 173-184.

Jossain, M. F. (2015). *Numerical modeling of Reinforced Comcrete Members Under Impact Load* . Bangladesh .

Leonardo M.Massone, B. L. (2017). Load-Deformation responses of slender structural steel reinforced concrete walls . *ELSEVIER*, 77-88.

Leonardo M.MASSONE, K. O. (2004). FLEXURAL AND SHEAR RESPONSES IN SLENDER RC SHEAR WALLS . *13th World Conference On Earthquake Engineering* (Pp. 1-4). Vancouver,B.C,Canada .

M.A. Osman, F. a. (2011). Behavior of shear walls under axial load and cyclic load. *Journal of Engineering sccieces ,Assiut University*, 933-946.

R.E.S Ismail, A. F. (2015). Finite Element Modeling of Partially Composited Castellated Beams. *Communication of Applied Electronics*.

W.Wallace, J. H. (1986). *Dispalacement-Based Design of Reinforced Concrete Structural Walls: An Experimental Investigation of walls with Rectangular and T-Shaped Cross-Sections.* USA: Earthquake Eng.Res.Ctr.Library .

W.Wallace, J. H. (1995). *Displacement-Based Design of Reinforced Concrete Structural Walls: An Experimental Investigation of Walls with Rectangular and T-shaped Cross-Sections.* California: National Science Foundation.

Ying Zhou, X. L. (2010). Seismic behaviour of composite shear walls with multi-embedded steel sections. Part I: experiment. *The Structural Design of Tall and Special Buildings* , 618-636.

Yusuf Sumer, M. A. (2015). Defining Parameters for concrete damage plasticity model . *Challenge Journal of Structural Mechanics 1*, 149-155.

Appendix A

The damage parameter of Concrete used for modelling is given on the following table

Table 3.1: damage parameter of Concrete used for modeling

Characteristic strength of concrete 34.5

Compression Behavior		**Compression damage**	
Yield stress	Inelastic strain	Damage Parameter	Cracking strain
14.12412327	0	0	1.50682E-005
25.63842771	0.000106991	0	0.000106991
34.34459719	0.000281609	0	0.000281609
40.02370041	0.000545369	0	0.000545369
42.5	0.000986645	0	0.000986645
42.49726871	0.001003526	6.42657E-005	0.001003526
41.30495368	0.001369638	0.028118737	0.001369638
36.33906281	0.001946875	0.144963228	0.001946875
27.20188413	0.00264695	0.359955668	0.00264695
25.80009055	0.00274023	0.392939046	0.00274023
Tension Behavior		**Tension Damage**	
Yield stress	Cracking strain	Damage Parameter	Cracking Strain
3.179318117	0	0	0
2.613832036	0.025140229	0.177863951	0.025140229
2.048345956	0.050269275	0.355727901	0.050269275
1.482859876	0.075374342	0.533591852	0.075374342
0.917373795	0.100411089	0.711455802	0.100411089
0.635863623	0.112792824	0.8	0.112792824
0.618115129	0.118277015	0.805582485	0.118277015
0.582772249	0.12919534	0.816698981	0.12919534
0.547429369	0.140109894	0.827815478	0.140109894
0.512086489	0.151019896	0.838931975	0.151019896

0.476743609	0.161924334	0.850048472	0.161924334
0.441400729	0.172821871	0.861164969	0.172821871
0.406057849	0.183710705	0.872281466	0.183710705
0.370714969	0.194588347	0.883397963	0.194588347
0.335372089	0.205451259	0.89451446	0.205451259
0.300029209	0.216294236	0.905630957	0.216294236
0.264686329	0.227109291	0.916747454	0.227109291
0.229343449	0.237883515	0.927863951	0.237883515
0.194000569	0.248594594	0.938980447	0.248594594
0.158657689	0.259200329	0.950096944	0.259200329
0.123314809	0.269610142	0.961213441	0.269610142
0.087971929	0.279587897	0.972329938	0.279587897
0.052629049	0.288263152	0.983446435	0.288263152
3.179318117	0	0	0

Characteristic strength of concrete 50

Compression Behavior		**Compression damage**	
Yield stress	Inelastic strain	Damage Parameter	Cracking strain
0	0	0	0
17.81620166	7.24697E-05	0	7.24697E-05
22.70383344	0.000150245	0	0.000150245
29.5329503	0.000367155	0	0.000367155
33.43550028	0.000675811	0	0.000675811
34.5	0.001016519	0	0.001016519
32.17745652	0.001646251	0.067320101	0.001646251
30.96409879	0.001815289	0.10248989	0.001815289
28.44371288	0.002108302	0.175544554	0.002108302
21.03359661	0.002788606	0.390330533	0.002788606
Tension Behavior		**Tension Damage**	
Yield stress	Cracking strain	Damage Parameter	Cracking Strain
2.66656293	0	0	0
2.254595043	0.021029441	0.154493968	0.021029441
1.842627155	0.042052051	0.308987936	0.042052051
1.430659268	0.063061931	0.463481903	0.063061931
0.533312586	0.108639273	0.8	0.108639273

0.537900768	0.106737874	0.798279365	0.106737874
0.512152775	0.117407334	0.807935238	0.117407334
0.486404782	0.128074589	0.817591111	0.128074589
0.460656789	0.138739268	0.827246984	0.138739268
0.434908796	0.149400914	0.836902857	0.149400914
0.409160803	0.160058955	0.84655873	0.160058955
0.38341281	0.170712663	0.856214603	0.170712663
0.357664817	0.181361104	0.865870476	0.181361104
0.331916824	0.192003051	0.875526349	0.192003051
0.306168831	0.202636867	0.885182222	0.202636867
0.280420838	0.213260311	0.894838095	0.213260311
0.254672845	0.223870237	0.904493968	0.223870237
0.228924852	0.234462084	0.914149841	0.234462084
0.203176859	0.24502898	0.923805714	0.24502898
0.187728063	0.25135287	0.929599238	0.25135287
0.177428866	0.255560061	0.933461587	0.255560061
0.151680873	0.266037089	0.94311746	0.266037089
0.022940908	0.31124135	0.991396825	0.31124135

APPENDIX B Input File

```
*Heading
** Job name: CYCLICNEW Model name: cyclic
** Generated by: Abaqus/CAE 6.13-1
*Preprint, echo=NO, model=NO, history=NO, contact=NO
**
** PARTS
**
*Part, name=closedphi6
*End Part
**
*Part, name=concrete
*End Part
**
*Part, name=horhoop
*End Part
**
*Part, name=i-section
*End Part
**
*Part, name=phi9longt
*End Part
**
*Part, name=phi9transvers
*End Part
**
*Part, name=phi12
*End Part
**
*Part, name=verthoop
*End Part
**
**
** ASSEMBLY
**
*Assembly, name=Assembly
**
*Instance, name=closedphi6-1, part=closedphi6
        25.,         25.,        -87.
        25.,         25.,        -87.,         26.,         25.,        -87.,         90.
*Node
      1,          0.,         62.,          0.
      2,        203.,         62.,          0.
      3,        203.,        -40.,          0.
      4,          0.,        -40.,          0.
*Element, type=T3D2H
1, 2, 1
2, 3, 2
3, 4, 3
4, 1, 4
*Nset, nset=Set-1, generate
 1,  4,  1
*Elset, elset=Set-1, generate
 1,  4,  1
** Section: phi6
*Solid Section, elset=Set-1, material="REINFORCEMENT BAR"
32.17,
```

```
*End Instance
**
*Instance, name=concrete-1, part=concrete
        0.,          0.,        -20.
        0.,          0.,        -20.,        -1.,          0.,        -20.,         90.
*Node
      1,          0.,        -20.,       4880.
      2,          0.,         56.,       4880.
      3,          0.,        132.,       4880.
;
Deleted for the sake of space…………………….

*Element, type=C3D8R
  1,  151,  152,  155,  154,   1,   2,   5,   4
  2,  152,  153,  156,  155,   2,   3,   6,   5
  3,  154,  155,  158,  157,   4,   5,   8,   7

*Nset, nset=Set-1, generate
   1,  1950,    1
*Elset, elset=Set-1, generate
   1,  1176,    1
** Section: conc
*Solid Section, elset=Set-1, material=CONCRETE
,
*End Instance
**
*Instance, name=horhoop-1, part=horhoop
     100.34,    21.203867,        -25.
*Node
      1,   10.4319334,   21.8980656,           0.
      2,  -7.67000008,    3.7961328,           0.
      3,          60.,    3.7961328,           0.
      4,   41.8980675,   21.8980656,           0.
*Element, type=T3D2H
1, 2, 1
2, 2, 3
3, 3, 4
*Nset, nset=Set-1, generate
 1,  4,  1
*Elset, elset=Set-1, generate
 1,  3,  1
** Section: phi6
*Solid Section, elset=Set-1, material="REINFORCEMENT BAR"
32.17,
*End Instance
**
*Instance, name=phi9longt-1, part=phi9longt
       304.,       4775.,        -25.
*Node
      1,          0.,       -4775.,           0.
      2,          0.,   -4572.7085,           0.
      3,          0.,   -4370.4165,           0.
      4,          0.,    -4168.125,           0.
      5,          0.,  -3965.83325,           0.
      6,          0.,  -3763.54175,           0.
*Nset, nset=Set-1, generate
  1,  25,   1
*Elset, elset=Set-1, generate
```

```
 1,  24,   1
** Section: phi9
*Solid Section, elset=Set-1, material="REINFORCEMENT BAR"
70.88,
*End Instance
**
*Instance, name=phi9transvers-1, part=phi9transvers
      935.,         25.,        -23.
      935.,         25.,        -23.,        936.,         25.,        -23.,         90.
*Node
      1,       -850.,        -40.,          0.
      2,       -850.,         -2.,          0.
      3,        200.,         -2.,          0.
      4,        200.,        -40.,          0.
      5,       -640.,         -2.,          0.
      6,       -430.,         -2.,          0.
      7,       -220.,         -2.,          0.
      8,        -10.,         -2.,          0.
*Element, type=T3D2H
1, 1, 2
2, 2, 5
3, 5, 6
4, 6, 7
5, 7, 8
6, 8, 3
7, 3, 4
*Nset, nset=Set-1, generate
 1,  8,  1
*Elset, elset=Set-1, generate
 1,  7,  1
** Section: phi9
*Solid Section, elset=Set-1, material="REINFORCEMENT BAR"
70.88,
*End Instance
**
*Instance, name=phi12-1, part=phi12
        25.,       4775.,        -25.
*Node
      1,          0.,      -4775.,          0.
      2,          0.,   -4572.7085,          0.
*Nset, nset=Set-1, generate
 1,  25,   1
*Elset, elset=Set-1, generate
 1,  24,   1
** Section: reinfphi12
*Solid Section, elset=Set-1, material="REINFORCEMENT BAR"
126.67,
*End Instance
**
*Instance, name=verthoop-1, part=verthoop
   88.873867,         25.,        -67.
   88.873867,         25.,        -67.,    89.873867,         25.,        -67.,         90.
*Node
      1,   21.8980656,   23.8980656,          0.
      2,    3.7961328,         42.,          0.
      3,    3.7961328,        -60.,          0.
      4,   21.8980656,  -41.8980675,          0.
*Element, type=T3D2H
```

```
1, 2, 1
2, 2, 3
3, 3, 4
*Nset, nset=Set-1, generate
 1,  4,  1
*Elset, elset=Set-1, generate
 1,  3,  1
** Section: phi6
*Solid Section, elset=Set-1, material="REINFORCEMENT BAR"
32.17,
*End Instance
**
*Instance, name=i-section-1, part=i-section
      51.57,        4855.,      -26.049
      51.57,        4855.,      -26.049,        52.57,        4855.,      -26.049,          90.
*Node
      1,   4.32000017,  -52.1399994,        4855.
      2,   4.32000017,        -100.,        4855.
      3,   4.32000017,        -100.,           0.
      4,   4.32000017,  -52.1399994,           0.
      5…

*Nset, nset=Set-1, generate
   1,  400,    1
*Elset, elset=Set-1, generate
   1,  168,    1
** Section: isec
*Solid Section, elset=Set-1, material="STRUCTURAL STEEL"
,
*End Instance
**
*Instance, name=phi9transvers-2, part=phi9transvers
       935.,          25.,        -129.
       935.,          25.,        -129.,         934.,          25.,        -129.,          90.
*Node
      1,        -850.,         -40.,           0.
      2,        -850.,          -2.,           0.
      3,         200.,          -2.,           0.
      4,         200.,         -40.,           0.
      5,        -640.,          -2.,           0.
      6,        -430.,          -2.,           0.
      7,        -220.,          -2.,           0.
      8,         -10.,          -2.,           0.
*Element, type=T3D2H
1, 1, 2
2, 2, 5
3, 5, 6
4, 6, 7
5, 7, 8
6, 8, 3
7, 3, 4
*Nset, nset=Set-1, generate
 1,  8,  1
*Elset, elset=Set-1, generate
 1,  7,  1
** Section: phi9
*Solid Section, elset=Set-1, material="REINFORCEMENT BAR"
70.88,
```

```
*End Instance
**
*Instance, name=verthoop-2, part=verthoop
    1127.33,    21.203867,        -67.
    1127.33,    21.203867,        -67., 1127.90735027955, 21.781217279552, -66.422649720448, 119.999999109416
*Node
      1,   21.8980656,   23.8980656,          0.
      2,    3.7961328,          42.,          0.
      3,    3.7961328,         -60.,          0.
      4,   21.8980656,  -41.8980675,          0.
*Element, type=T3D2H
1, 2, 1
2, 2, 3
3, 3, 4
*Nset, nset=Set-1, generate
 1,  4,  1
*Elset, elset=Set-1, generate
 1,  3,  1
** Section: phi6
*Solid Section, elset=Set-1, material="REINFORCEMENT BAR"
32.17,
*End Instance
**
*Instance, name=i-section-1-lin-2-1, part=i-section
    1018.57,        4855.,      -26.049
    1018.57,        4855.,      -26.049,     1019.57,        4855.,      -26.049,          90.
*Node
      1,   4.32000017,  -52.1399994,        4855.
      2,   4.32000017,        -100.,        4855.
      3,   4.32000017,        -100.,           0.
      4,   4.32000017,  -52.1399994,           0.
*Nset, nset=Set-1, generate
   1,  400,    1
*Elset, elset=Set-1, generate
   1,  168,    1
** Section: isec
*Solid Section, elset=Set-1, material="STRUCTURAL STEEL"
,
*End Instance
**
*Instance, name=closedphi6-1-lin-1-2, part=closedphi6
        25.,         127.,         -87.
        25.,         127.,         -87.,          26.,         127.,         -87.,          90.
*Node
      1,           0.,          62.,           0.
      2,         203.,          62.,           0.
      3,         203.,         -40.,           0.
      4,           0.,         -40.,           0.
*Element, type=T3D2H
1, 2, 1
2, 3, 2
3, 4, 3
4, 1, 4
*Nset, nset=Set-1, generate
 1,  4,  1
*Elset, elset=Set-1, generate
 1,  4,  1
** Section: phi6
```

```
*Solid Section, elset=Set-1, material="REINFORCEMENT BAR"
32.17,
*End Instance
**
** Section: reinfphi12
*Solid Section, elset=Set-1, material="REINFORCEMENT BAR"
126.67,
*End Instance
**
*Instance, name=phi12-1-lin-2-1-1-lin-4-1, part=phi12
     991.99,       4775.,        -25.
*Node
      1,           0.,      -4775.,           0.
      2,           0.,   -4572.7085,           0.
      3,           0.,   -4370.4165,           0.
      4,           0.,    -4168.125,           0.
      5,           0.,  -3965.83325,           0.
      6,           0.,  -3763.54175,           0.
      7,           0.,    -3561.25,           0.
      8,           0.,  -3358.95825,           0.
      9,           0.,  -3156.66675,           0.
     10,           0.,    -2954.375,           0.
     11,           0.,  -2752.08325,           0.
     12,           0.,  -2549.79175,           0.
     13,           0.,     -2347.5,           0.
     14,           0.,  -2145.20825,           0.
     15,           0.,  -1942.91663,           0.
     16,           0.,    -1740.625,           0.
     17,           0.,  -1538.33337,           0.
     18,           0.,  -1336.04163,           0.
     19,           0.,    -1133.75,           0.
     20,           0.,  -931.458313,           0.
     21,           0.,  -729.166687,           0.
     22,           0.,    -526.875,           0.
     23,           0.,  -324.583344,           0.
     24,           0.,  -122.291664,           0.
     25,           0.,         80.,           0.
*Element, type=T3D2H
 1,  1,  2
 2,  2,  3
 3,  3,  4
 4,  4,  5
 5,  5,  6
 6,  6,  7
 7,  7,  8
 8,  8,  9
*Nset, nset=Set-1, generate
  1,  25,   1
*Elset, elset=Set-1, generate
  1,  24,   1
** Section: reinfphi12
*Solid Section, elset=Set-1, material="REINFORCEMENT BAR"
126.67,
*End Instance
**
*Instance, name=phi12-1-lin-2-1-1-lin-4-2, part=phi12
     991.99,       4775.,       -127.
*Node
```

```
     1,           0.,       -4775.,           0.
     2,           0.,   -4572.7085,           0.
     3,           0.,   -4370.4165,           0.
     4,           0.,    -4168.125,           0.
     5,           0.,  -3965.83325,           0.
     6,           0.,  -3763.54175,           0.
     7,           0.,     -3561.25,           0.
     8,           0.,  -3358.95825,           0.
     9,           0.,  -3156.66675,           0.
    10,           0.,    -2954.375,           0.
    11,           0.,  -2752.08325,           0.
    12,           0.,  -2549.79175,           0.
    13,           0.,      -2347.5,           0.
    14,           0.,  -2145.20825,           0.
    15,           0.,  -1942.91663,           0.
    16,           0.,    -1740.625,           0.
    17,           0.,  -1538.33337,           0.
    18,           0.,  -1336.04163,           0.
    19,           0.,     -1133.75,           0.
    20,           0.,  -931.458313,           0.
    21,           0.,  -729.166687,           0.
    22,           0.,     -526.875,           0.
    23,           0.,  -324.583344,           0.
    24,           0.,  -122.291664,           0.
    25,           0.,          80.,           0.
*Element, type=T3D2H
 1,  1,  2
 2,  2,  3
 3,  3,  4
 4,  4,  5
 5,  5,  6
 6,  6,  7
 7,  7,  8
 8,  8,  9
 9,  9, 10
10, 10, 11
11, 11, 12
12, 12, 13
13, 13, 14
14, 14, 15
15, 15, 16
16, 16, 17
17, 17, 18
18, 18, 19
19, 19, 20
20, 20, 21
21, 21, 22
22, 22, 23
23, 23, 24
24, 24, 25
*Nset, nset=Set-1, generate
  1,  25,   1
*Elset, elset=Set-1, generate
  1,  24,   1
** Section: reinfphi12
*Solid Section, elset=Set-1, material="REINFORCEMENT BAR"
126.67,
*End Instance
```

```
**
*Instance, name=phi12-1-lin-3-1-lin-1-2, part=phi12
     160.34,       4775.,       -127.
*Node
      1,           0.,      -4775.,           0.
      2,           0.,   -4572.7085,           0.
      3,           0.,   -4370.4165,           0.
      4,           0.,    -4168.125,           0.
      5,           0.,  -3965.83325,           0.
      6,           0.,  -3763.54175,           0.
      7,           0.,    -3561.25,           0.
      8,           0.,  -3358.95825,           0.
      9,           0.,  -3156.66675,           0.
     10,           0.,    -2954.375,           0.
     11,           0.,  -2752.08325,           0.
     12,           0.,  -2549.79175,           0.
     13,           0.,     -2347.5,           0.
     14,           0.,  -2145.20825,           0.
     15,           0.,  -1942.91663,           0.
     16,           0.,    -1740.625,           0.
     17,           0.,  -1538.33337,           0.
     18,           0.,  -1336.04163,           0.
     19,           0.,    -1133.75,           0.
     20,           0.,  -931.458313,           0.
     21,           0.,  -729.166687,           0.
     22,           0.,    -526.875,           0.
     23,           0.,  -324.583344,           0.
     24,           0.,  -122.291664,           0.
     25,           0.,         80.,           0.
*Element, type=T3D2H
 1,  1,  2
 2,  2,  3
 3,  3,  4
 4,  4,  5
 5,  5,  6
24, 24, 25
*Nset, nset=Set-1, generate
  1,  25,   1
*Elset, elset=Set-1, generate
  1,  24,   1
** Section: reinfphi12
*Solid Section, elset=Set-1, material="REINFORCEMENT BAR"
126.67,
*End Instance
**
*Instance, name=phi12-1-lin-3-1-lin-2-1, part=phi12
     228.01,       4775.,        -25.
*Node
      1,           0.,      -4775.,           0.
      2,           0.,   -4572.7085,           0.
      3,           0.,   -4370.4165,           0.
      4,           0.,    -4168.125,           0.
      5,           0.,  -3965.83325,           0.
      6,           0.,  -3763.54175,           0.
      7,           0.,    -3561.25,           0.
      8,           0.,  -3358.95825,           0.
      9,           0.,  -3156.66675,           0.
     10,           0.,    -2954.375,           0.
```

```
    11,          0.,  -2752.08325,          0.
    12,          0.,  -2549.79175,          0.
    13,          0.,      -2347.5,          0.
    14,          0.,  -2145.20825,          0.
    15,          0.,  -1942.91663,          0.
    16,          0.,    -1740.625,          0.
    17,          0.,  -1538.33337,          0.
    18,          0.,  -1336.04163,          0.
    19,          0.,     -1133.75,          0.
    20,          0.,  -931.458313,          0.
    21,          0.,  -729.166687,          0.
    22,          0.,     -526.875,          0.
    23,          0.,  -324.583344,          0.
    24,          0.,  -122.291664,          0.
    25,          0.,          80.,          0.
*Element, type=T3D2H
 1,  1,  2
 2,  2,  3
 3,  3,  4
 4,  4,  5
 5,  5,  6
 6,  6,  7
 7,  7,  8
 8,  8,  9
 9,  9, 10
10, 10, 11
11, 11, 12
12, 12, 13
13, 13, 14
14, 14, 15
15, 15, 16
16, 16, 17
17, 17, 18
18, 18, 19
19, 19, 20
20, 20, 21
21, 21, 22
22, 22, 23
23, 23, 24
24, 24, 25
*Nset, nset=Set-1, generate
  1,  25,   1
*Elset, elset=Set-1, generate
  1,  24,   1
** Section: reinfphi12
*Solid Section, elset=Set-1, material="REINFORCEMENT BAR"
126.67,
*End Instance
**
*Instance, name=phi12-1-lin-3-1-lin-2-2, part=phi12
     228.01,       4775.,       -127.
*Node
      1,          0.,       -4775.,          0.
      2,          0.,   -4572.7085,          0.
*Element, type=T3D2H
 1,  1,  2
 2,  2,  3
 3,  3,  4
```

```
*Nset, nset=Set-1, generate
 1,  25,   1
*Elset, elset=Set-1, generate
 1,  24,   1
** Section: reinfphi12
*Solid Section, elset=Set-1, material="REINFORCEMENT BAR"
126.67,
*End Instance
**
*Instance, name=phi9transvers-1-lin-1-2, part=phi9transvers
      935.,        177.,        -23.
      935.,        177.,        -23.,        936.,        177.,        -23.,         90.
*Node
      1,       -850.,        -40.,          0.
      2,       -850.,         -2.,          0.
      3,        200.,         -2.,          0.
      4,        200.,        -40.,          0.
      5,       -640.,         -2.,          0.
      6,       -430.,         -2.,          0.
      7,       -220.,         -2.,          0.
      8,        -10.,         -2.,          0.
*Element, type=T3D2H
1, 1, 2
2, 2, 5
3, 5, 6
4, 6, 7
5, 7, 8
6, 8, 3
7, 3, 4
*Nset, nset=Set-1, generate
 1,  8,  1
*Elset, elset=Set-1, generate
 1,  7,  1
** Section: phi9
*Solid Section, elset=Set-1, material="REINFORCEMENT BAR"
70.88,
*End Instance
**
*Nset, nset=Set-1, generate
 1,  8,  1
*Element, type=T3D2H
*Instance, name=verthoop-1-lin-1-2, part=verthoop
   88.873867,        127.,        -67.
   88.873867,        127.,        -67.,   89.873867,        127.,        -67.,         90.
*Node
      1,   21.8980656,   23.8980656,          0.
      2,    3.7961328,         42.,          0.
      3,    3.7961328,        -60.,          0.
      4,   21.8980656,  -41.8980675,          0.
*Element, type=T3D2H
1, 2, 1
**
*Instance, name=horhoop-1-lin-1-2, part=horhoop
      100.34,   123.203867,        -25.
*Node
      1,   10.4319334,   21.8980656,          0.
      2,  -7.67000008,    3.7961328,          0.
      3,         60.,    3.7961328,          0.
```

```
     4,   41.8980675,   21.8980656,          0.
*Element, type=T3D2H
1, 2, 1
2, 2, 3
3, 3, 4
*Nset, nset=Set-1, generate
 1,  4,  1
*Elset, elset=Set-1, generate
 1,  3,  1
** Section: phi6
*Solid Section, elset=Set-1, material="REINFORCEMENT BAR"
32.17,
*End Instance
**
*Instance, name=horhoop-1-lin-1-3, part=horhoop
     100.34,   225.203867,        -25.
*Node
     1,   10.4319334,   21.8980656,          0.
     2,  -7.67000008,    3.7961328,          0.
     3,          60.,    3.7961328,          0.
     4,   41.8980675,   21.8980656,          0.
*Element, type=T3D2H
1, 2, 1
2, 2, 3

** Section: phi9
*Solid Section, elset=Set-1, material="REINFORCEMENT BAR"
70.88,
*End Instance
**
*Instance, name=phi9longt-1-lin-3-2-lin-2-1, part=phi9longt
     763.99,       4775.,       -127.
*Node
     1,          0.,      -4775.,          0.
     2,          0.,     -4289.5,          0.
     3,          0.,      -3804.,          0.
     4,          0.,     -3318.5,          0.
     5,          0.,      -2833.,          0.
     6,          0.,     -2347.5,          0.
     7,          0.,      -1862.,          0.
     8,          0.,     -1376.5,          0.
     9,          0.,       -891.,          0.
    10,          0.,      -405.5,          0.
    11,          0.,         80.,          0.
*Element, type=T3D2H
 1,  1,  2
 2,  2,  3
 3,  3,  4
 4,  4,  5
 5,  5,  6
 6,  6,  7
 7,  7,  8
 8,  8,  9
 9,  9, 10
10, 10, 11
*Nset, nset=Set-1, generate
  1,  11,   1
*Elset, elset=Set-1, generate
```

```
 1,  10,   1
** Section: phi9
*Solid Section, elset=Set-1, material="REINFORCEMENT BAR"
70.88,
*End Instance
**
*Instance, name=phi9longt-1-lin-3-2-lin-3-1, part=phi9longt
     915.99,       4775.,       -127.
*Node
      1,           0.,      -4775.,           0.
      2,           0.,     -4289.5,           0.
      3,           0.,      -3804.,           0.
      4,           0.,     -3318.5,           0.
      5,           0.,      -2833.,           0.
      6,           0.,     -2347.5,           0.
      7,           0.,      -1862.,           0.
      8,           0.,     -1376.5,           0.
      9,           0.,       -891.,           0.
     10,           0.,      -405.5,           0.
     11,           0.,         80.,           0.
*Element, type=T3D2H
 1,  1,  2
 2,  2,  3
 3,  3,  4
 4,  4,  5
 5,  5,  6
 6,  6,  7
 7,  7,  8
 8,  8,  9
 9,  9, 10
10, 10, 11
*Nset, nset=Set-1, generate
 1,  11,   1
*Elset, elset=Set-1, generate
 1,  10,   1
** Section: phi9
*Solid Section, elset=Set-1, material="REINFORCEMENT BAR"
70.88,
*End Instance
**
*Node
      1,       1300.,       4880.,         -76.
*Nset, nset=Boundary2, instance=concrete-1
  148,  149,  150,  298,  299,  300,  448,  449,  450,  598,  599,  600,  748,  749,  750,  898
  899,  900, 1048, 1049, 1050, 1198, 1199, 1200, 1348, 1349, 1350, 1498, 1499, 1500, 1648, 1649
 1650, 1798, 1799, 1800, 1948, 1949, 1950
*Nset, nset=Boundary2, instance=i-section-1
  1,  2,  5,  8, 10, 11, 13, 15, 18, 19, 21, 23, 25, 28, 29, 32
*Nset, nset=Boundary2, instance=i-section-1-lin-2-1
  1,  2,  5,  8, 10, 11, 13, 15, 18, 19, 21, 23, 25, 28, 29, 32
*Elset, elset=Boundary2, instance=concrete-1
   97,   98,  195,  196,  293,  294,  391,  392,  489,  490,  587,  588,  685,  686,  783,  784
  881,  882,  979,  980, 1077, 1078, 1175, 1176
*Elset, elset=Boundary2, instance=i-section-1
   1,  48,  72,  96,  97, 121, 145
*Elset, elset=Boundary2, instance=i-section-1-lin-2-1
   1,  48,  72,  96,  97, 121, 145
*Nset, nset=Set-6, instance=concrete-1
```

```
 1, 3
*Nset, nset=Set-7, instance=concrete-1, generate
 1801,  1803,     1
*Elset, elset=Set-7, instance=concrete-1
 1079, 1080
n-1-2, generate
 1,  3,  1

*Elset, elset=_s_Surf-6_S3, internal, instance=concrete-1
   1,   2,   99,  100,  197,  198,  295,  296,  393,  394,  491,  492,  589,  590,  687,  688
 785,  786,  883,  884,  981,  982, 1079, 1080
*Surface, type=ELEMENT, name=s_Surf-6
_s_Surf-6_S3, S3
*Elset, elset=_s_Surf-7_S3, internal, instance=concrete-1
   1,   2,   99,  100,  197,  198,  295,  296,  393,  394,  491,  492,  589,  590,  687,  688
 785,  786,  883,  884,  981,  982, 1079, 1080
*Surface, type=ELEMENT, name=s_Surf-7
_s_Surf-7_S3, S3
** Constraint: Constraint-2
*Coupling, constraint name=Constraint-2, ref node=m_Set-23, surface=s_Surf-7
*Kinematic
** Constraint: Constraint-embed
*Embedded Element, host elset=s_Set-11
m_Set-11
*End Assembly
*Amplitude, name=Amp-1
          0.,           0.,    0.011904762,         0.025,    0.023809524,           0.,    0.035714286,        -0.025
   0.047619048,           0.,     0.05952381,        0.025,    0.071428571,           0.,    0.083333333,        -0.025
   0.095238095,           0.,    0.107142857,         0.05,    0.119047619,           0.,    0.130952381,         -0.05
   0.142857143,           0.,    0.154761905,         0.05,    0.166666667,           0.,    0.178571429,         -0.05
    0.19047619,           0.,    0.202380952,        0.125,    0.214285714,           0.,    0.226190476,        -0.125
   0.238095238,           0.,           0.25,        0.125,    0.261904762,           0.,    0.273809524,        -0.125
   0.285714286,           0.,    0.297619048,        0.125,     0.30952381,           0.,    0.321428571,        -0.125
   0.333333333,           0.,    0.345238095,       0.1875,    0.357142857,           0.,    0.369047619,       -0.1875
   0.380952381,           0.,    0.392857143,       0.1875,    0.404761905,           0.,    0.416666667,       -0.1875
   0.428571429,           0.,     0.44047619,         0.25,    0.452380952,           0.,    0.464285714,         -0.25
   0.476190476,           0.,    0.488095238,         0.25,            0.5,           0.,    0.511904762,         -0.25
   0.523809524,           0.,    0.535714286,        0.375,    0.547619048,           0.,     0.55952381,        -0.375
   0.571428571,           0.,    0.583333333,        0.375,    0.595238095,           0.,    0.607142857,        -0.375
   0.619047619,           0.,    0.630952381,          0.5,    0.642857143,           0.,    0.654761905,          -0.5
   0.666666667,           0.,    0.678571429,          0.5,     0.69047619,           0.,    0.702380952,          -0.5
   0.714285714,           0.,    0.726190476,        0.625,    0.738095238,           0.,           0.75,        -0.625
   0.761904762,           0.,    0.773809524,        0.625,    0.785714286,           0.,    0.797619048,        -0.625
    0.80952381,           0.,    0.821428571,         0.75,    0.833333333,           0.,    0.845238095,         -0.75
   0.857142857,           0.,    0.869047619,         0.75,    0.880952381,           0.,    0.892857143,         -0.75
   0.904761905,           0.,    0.916666667,           1.,    0.928571429,           0.,     0.94047619,           -1.
   0.952380952,           0.,    0.964285714,           1.,    0.976190476,           0.,    0.988095238,           -1.
          1.,           0.
*Amplitude, name=axial
          0.,           1.,         0.01,           1.,           1.,           1.
**
** MATERIALS
**
*Material, name=CONCRETE
*Density
 2.4e-09,
*Elastic
 31898.4, 0.2
```

```
*Concrete Damaged Plasticity
38.,  0.1, 1.16, 0.67,   0.
*Concrete Compression Hardening
 17.8162,         0.
 22.7038, 0.000150245
  29.533, 0.000367155
 33.4355, 0.000675811
    34.5,  0.00101652
 32.1775,  0.00164625
 30.9641,  0.00181529
 28.4437,   0.0021083
 21.0336,  0.00278861
 19.9886,  0.00287337
*Concrete Tension Stiffening
  2.66656,        0.
   2.2546, 0.0210294
  1.84263, 0.0420521
  1.43066, 0.0630619
 0.533313,  0.108639
 0.512153,  0.117407
 0.486405,  0.128075
 0.460657,  0.138739
 0.434909,  0.149401
 0.409161,  0.160059
 0.383413,  0.170713
 0.357665,  0.181361
 0.331917,  0.192003
 0.306169,  0.202637
 0.280421,   0.21326
 0.254673,   0.22387
 0.228925,  0.234462
 0.203177,  0.245029
 0.187728,  0.251353
 0.177429,   0.25556
 0.151681,  0.266037
0.0229409,  0.311241
*Concrete Compression Damage
       0.,         0.
       0., 7.24697e-05
       0., 0.000150245
       0., 0.000367155
       0., 0.000675811
       0.,  0.00101652
0.0673201,  0.00164625
  0.10249,  0.00181529
 0.175545,   0.0021083
 0.390331,  0.00278861
 0.420619,  0.00287337
*Concrete Tension Damage
      0.,       0.
 0.154494, 0.0210294
 0.308988, 0.0420521
 0.463482, 0.0630619
      0.8,  0.108639
 0.807935,  0.117407
 0.817591,  0.128075
 0.827247,  0.138739
 0.836903,  0.149401
```

```
 0.846559,  0.160059
 0.856215,  0.170713
  0.86587,  0.181361
 0.875526,  0.192003
 0.885182,  0.202637
 0.894838,   0.21326
 0.904494,   0.22387
  0.91415,  0.234462
 0.923806,  0.245029
 0.929599,  0.251353
 0.933462,   0.25556
 0.943117,  0.266037
 0.991397,  0.311241
*Material, name="REINFORCEMENT BAR"
*Density
 7.6e-09,
*Elastic
200000., 0.3
*Plastic
413.,   0.
600., 0.06
*Material, name="STRUCTURAL STEEL"
*Density
 7.6e-09,
*Elastic
200000., 0.3
*Plastic
400.,    0.
400., 0.028
500.,  0.09
**
** BOUNDARY CONDITIONS
**
** Name: BC-1 Type: Symmetry/Antisymmetry/Encastre
*Boundary
boundary, ENCASTRE
** ----------------------------------------------------------------
**
** STEP: Step-1
**
*Step, name=Step-1, nlgeom=YES, inc=2000
*Static, stabilize, allsdtol=0.05, continue=YES
0.01, 1., 1e-07, 1.
**
** BOUNDARY CONDITIONS
**
** Name: BC-2 Type: Displacement/Rotation
*Boundary, amplitude=Amp-1
Set-24, 1, 1, 180.
**
** LOADS
**
** Name: pressure   Type: Pressure
*Dsload, amplitude=axial
loadsur, P, 6.91329
**
** OUTPUT REQUESTS
**
```

```
*Restart, write, overlay, frequency=1
**
** FIELD OUTPUT: F-Output-1
**
*Output, field
*Node Output
CF, RF, U
*Element Output, directions=YES
DAMAGEC, DAMAGET, LE, PE, PEEQ, PEMAG, S
*Contact Output
CDISP, CSTRESS
**
** HISTORY OUTPUT: H-Output-1
**
*Output, history, variable=PRESELECT
*End Step
```